Abelian and non-Abelian strings

A THESIS
SUBMITTED TO THE FACULTY OF THE GRADUATE SCHOOL
OF THE UNIVERSITY OF MINNESOTA
BY

Sergey Monin

IN PARTIAL FULFILLMENT OF THE REQUIREMENTS
FOR THE DEGREE OF
DOCTOR OF PHILOSOPHY

MIKHAIL SHIFMAN

June, 2017

Acknowledgements

I would like to take this opportunity and thank the people who helped me with my project. I would like to thank my Adviser, Professor Mikhail Shifman for working with me on the problems, for providing suggestions and for insightful discussions. I have learned a lot from Professor Shifman during the course of our interactions. Also, I would like to thank Professor Alexei Yung, who also worked on the problems, for very useful discussions and for providing suggestions. It was a was an honour to work with both of them.

Dedication

To my family

Abstract

We study world-sheet theories of Abelian and non-Abelian strings that arise in different models. Considering a model in which Abelian (Abrikosov-Nielsen-Olesen) string acquires rotational (quasi)moduli we analyze the parameter space to find examples in which these strings not only coexist but are degenerate in tension. We prove that both solutions are locally stable, i.e there are no negative modes in the string background. The tension degeneracy is achieved at the classical level and is expected to be lifted by quantum corrections. Moreover, using a representative set of parameters we numerically calculate the low-energy Lagrangian on the world sheet of the Abrikosov-Nielsen-Olesen string. The bulk model is deformed by a spin-orbit interaction generating a number of "entangled" terms on the string world sheet.

We also consider modifications of $\mathcal{N} = 2$ supersymmetric QCD with the U(N) gauge group and $N_f = N$ quark flavors. These models support non-Abelian strings. The dynamics of the orientational modes is described by two-dimensional CP($N-1$) model with varying degrees of supersymmetry. We used analytical methods to solve the CP($N-1$) model at finite string length L assuming periodic boundary conditions.

In the pure bosonic theory in the large-N limit we detect a phase transition at $L \sim \Lambda_{\rm CP}^{-1}$ (which is expected to become a rapid crossover at finite N). At large L the CP($N-1$) model develops a mass gap and is in the Coulomb/confinement phase, while at small L it is in the deconfinement phase. In the $\mathcal{N} = (2,2)$ supersymmetric CP($N-1$) model at finite L we find a large-N solution which was not known previously. We use the power of holomorphy to deduce that the theory has a single phase independently of the value of $L\Lambda_{\rm CP}$. For any value of this parameter a mass gap develops and supersymmetry remains unbroken. So does the $SU(N)$ symmetry of the target space. In the heterotic $\mathcal{N} = (0,2)$ CP($N-1$) model we find a rich phase structure and discuss how it matches the $\mathcal{N} = (2,2)$ limit.

Contents

List of Tables

List of Figures

Chapter 1

Introduction

Quark confinement in QCD is a long-standing problem in Physics. The attraction force between a quark and antiquark does not decrease with distance. Instead the potential energy of their interaction grows linearly. Thus quarks never appear as free particles, and one can only observe mesons and baryons.

A similar phenomenon occurs in superconductors of the second type and is referred to as the Meissner effect. Consider a superconducting sample with magnets attached to it on opposite sides. On one hand magnetic field cannot penetrate into a superconductor. On the other hand the flux of magnetic field must be conserved. Thus, a flux tube forms between the magnets preserving the flux of magnetic field. Moreover, the superconductivity is destroyed inside the flux tube. Since the flux tube has constant tension the potential between two magnets growns linearly with distance. The flux tube described above is referred to as ANO (Abrikosov, Nielsen and Olesen) string [1]. However, it cannot explain the confinement of quarks in QCD, since it is a chromomagnetic flux tube an not a chromoelectric one.

A dual Meissner effect was suggested by t Hooft and Mandelstam [2] to explain the confinement. They conjectured that due to color magnetic-monopole condensation the non-Abelian flux tube forms between the quarks. The Seiberg-Witten solution [3] of $\mathcal{N} = 2$ supersymmetric Yang-Mills theory demonstrated the existence of massless monopoles which can condense, leading to the formation of ANO flux tube. It carries chromoelectric flux, but is still Abelian.

Genuinly non-Abelian strings were first found in $\mathcal{N} = 2$ supersymmetric gauge

theories [4, 5, 6, 7]. Later this construction was generalized to a wide class of non-Abelian gauge theories, both supersymmetric and non-supersymmetric, see [8, 9, 10, 11]. Both Abelian and non-Abelian strings have translational modes associated with broken translation symmetries. The main feature of the non-Abelian strings is the occurrence of extra moduli: orienational zero modes associated with the color flux rotation in the internal space.

In this thesis I present the study of Abelian and non-Abelian strings arising in two different models. The thesis is organised as follows: In Chapter (2) we consider a simple model with "spin-orbit" interactions supporting the Abrikosov-Nielsen-Olesen (ANO) [1] or similar strings (vortices) with "extra" non-Abelian moduli (or quasimoduli) on the string world sheet. Such extra moduli fields can appear in the bulk models that have order parameters carrying spatial indices, such as those relevant for superfluidity in ^{3}He (see e.g. [12]). This particular example was studied in [13], which, in fact inspired a more detailed numerical analysis presented below. The studies in [14, 13, 15] were carried out at a qualitative level. Here we perform calculations needed for the proof of stability of the relevant solutions and derivation of all constants appearing in the low-energy theory on the string world sheet.

First, we will consider the simplest model [14] assuming weak coupling in the bulk (to justify the quasiclassical approximation), determine the profile functions to find the string solution, and derive the world sheet model. The general theory of the string moduli in the absence of the spin-orbit terms is discussed in [16, 17].

Then we introduce a spin-orbit interaction in the bulk. The impact of this interaction on the string (vortex) world sheet amounts to lifting all or some rotational zero modes (i.e. those not associated with the spontaneous breaking of the translational symmetry by the string). However, under certain condition on a parameter determining the spin-orbit interaction in the bulk, the mass gap generated on the world sheet remains small, and the extra zero modes survive as quasizero modes (some may remain at zero at the classical level). In addition to the above mode-lifting, the spin-orbit interaction generates a number of interesting entangled terms on the string world sheet which couple rotational and translational modes (despite the fact that the translational modes remain exactly gapless).

In Chapters 3 and 4 we consider a differenct model supporting non-Abelian strings

[18]. As was mentioned the main feature of the non-Abelian strings is the occurrence of orienational zero modes associated with their color flux rotation in the internal space. Dynamics of these orientational moduli in the model we consider in Chapters 3 and 4 is described by two-dimensional CP($N-1$) model on the string world-sheet.

Recently there was a considerable progress in the study of long confining strings of a fixed length both on lattices [19, 20] and by constructing the effective theory on the string world sheet, see [21, 22]. The energy of the Abrikosov-Nielsen-Olesen (ANO) closed string [1] in the Abelian-Higgs model as a function of the string length L (in the large-L limit) can be written as

$$E(L) = TL - \frac{\gamma}{L} + \frac{c_3}{TL^3} + \cdots , \tag{1.0.1}$$

where T is the string tension and ellipses stand for terms of the higher order in $1/L$. This $1/L$ expansion is determined by the low-energy effective two-dimensional theory on the string world-sheet. For the ANO string the world-sheet theory is given by the Nambu-Goto action plus higher derivative corrections. It is plausible to assume that a similar structure applies to QCD confining strings. Recently a significant progress occurred in measuring the spectrum of long confining QCD strings in lattice simulations, see, for example, [23].

The $1/L$ term in (1.0.1) is referred to as the Lüscher term [24]. The coefficient γ is universal. Its value is determined by the number of massless (light) degrees of freedom on the string world-sheet. The Abelian strings possess only two massless excitations due to two translational zero modes; the Lüscher term is, correspondingly, $\gamma = \pi/3$.

In Chapters 3 and 4 we study the L dependence of $E(L)$ for all values of L, large and small (see below), taking account of the orientational moduli that are described by two-dimensional CP($N-1$) model. The latter is asymptotically free and develops its own dynamical scale $\Lambda_{\rm CP}$. This modifies the expansion in (1.0.1). Assuming that

$$\Lambda_{\rm CP} \ll \sqrt{T} \tag{1.0.2}$$

we can write

$$E(L) = TL + \frac{f(\Lambda_{CP}L)}{L} + O\left(\frac{1}{TL^3}\right). \tag{1.0.3}$$

In Chapters 3 and 4 we present a detailed calculation of the string energy for strings

with

$$L \gg 1/\sqrt{T}\,. \tag{1.0.4}$$

For these values of L higher derivative corrections to the effective world-sheet theory can be ignored, and we use CP($N-1$)-based description to calculate the function $f(\Lambda_{CP}L)$ (which is already known [25] in the limits $L \gg \Lambda_{\rm CP}^{-1}$ and $L \ll \Lambda_{\rm CP}^{-1}$). We solve the CP($N-1$) model using the large-$N$ approximation [26] and imposing periodic boundary conditions (on the boson and fermion fields in the case of supersymmetric model, see below).

Now, when we have two free parameters in the problem under consideration, N and L, and both can be large, the ordering of taking limits is of paramount importance and a source of a number of paradoxes. We will *always* take first the limit $N \to \infty$. In this limit the number of dynamical degrees of freedom is infinite (even in the quantum-mechanical limit $L \to 0$) and, moreover, all interactions die off. This makes possible phase transitions.

In Chapter 3 we study both non-supersymmetric case as well as 1/2-BPS string in $\mathcal{N} = 2$ supersymmetric QCD. For non-supersymmetric case we find a phase transition in the world-sheet theory in the $N = \infty$ limit. At large L this theory develops a mass gap and is in the Coulomb/confinement phase. Finite-length effects coming from orientational moduli are exponentially suppressed. We find that at $L \gg \Lambda_{\rm CP}$

$$f(\Lambda_{CP}L) = -\frac{\pi}{3} - N\sqrt{\frac{2}{\pi}}\,\sqrt{\Lambda_{\rm CP}L}\,e^{-\Lambda_{\rm CP}L} + \cdots\,, \tag{1.0.5}$$

where the first term is the conventional Lüscher term coming from the translational moduli.

At small length the CP($N-1$) model is in the deconfinement phase. Massless orientational moduli contribute to the Lüscher term which becomes dependent on the rank of the bulk gauge group. At $\sqrt{T} \ll L \ll \Lambda_{\rm CP}$ we find that

$$f(\Lambda_{\rm CP}L) = -N\,\frac{\pi}{3}. \tag{1.0.6}$$

Next, we study supersymmetric case considering BPS-saturated non-Abelian string in four-dimensional $\mathcal{N} = 2$ SQCD. In this case the world-sheet theory for orientational

modes is $\mathcal{N}=(2,2)$ supersymmetric CP$(N-1)$ model. Solving this theory in the large-N limit we find a *single* phase with unbroken supersymmetry and a mass gap. The mass gap turns out to be independent of the string length. The chiral Z_{2N} symmetry is broken down to Z_2, in much the same way as for infinitely long string. The photon field acquires a mass term, and no Coulomb/confining potential is generated. Instead, the theory has N degenerate vacua representing N elementary strings. The Lüscher term vanishes due to the boson-fermion cancellation.

In Chapter (4) we introduce a mass term for the adjoint matter in the bulk and break $\mathcal{N}=2$ supersymmetry down to $\mathcal{N}=1$. The string remains BPS saturated [27]. It was conjectured by Edalati and Tong [28] and confirmed in [29] that the target space in the deformed model is $CP(N-1)\times C$. The right-handed supertranslational modes become coupled to superorientational ones, and the world sheet theory becomes heterotic model with $\mathcal{N}=(0,2)$ supersymmetry. It is important that this is a nonminimal model (cf. [30]) well defined for all N.

We solve the above heterotic $\mathcal{N}=(0,2)$ CP$(N-1)$ model on a cylinder with circumference L in the large-N approximation, assuming periodic boundary conditions. We observe three distinct phases. Two phases (III and IV in Fig. 1) preserve the SU(N) global symmetry. The finite-L effects are exponentially suppressed at large L and intermediate values of the deformation parameter u, in much the same way as in non-supersymmetric theory considered in Chapter 3. The parameter of deformation u is related to the mass of the adjoint field in the bulk SQCD.

The theory in phase (IV) has mass gap and N vacua; the discrete chiral Z_{2N} symmetry is spontaneously broken down to Z_2. As we increase u still keeping L large the theory undergoes a third order phase transition into a phase (III) with a single vacuum and unbroken Z_{2N}. This is a phase with massless fermions.

As is the case for non-supersymmetric theory, we find a phase (II) with would-be broken SU(N) symmetry at small L. In the latter phase a mass gap is zero in the leading approximation. Moreover, we find that the vacuum energy also vanishes at $N=\infty$. We expect corrections of higher order in $1/N$ (or, perhaps, exponential corrections e^{-N}) to break $\mathcal{N}=(0,2)$ supersymmetry and lift the vacuum energy. We stress that SU(N) is broken only when $N=\infty$. At large but finite N this and other phase transitions turn into rapid crossovers.

We also discuss how this rich phase structure evolves to the $\mathcal{N} = (2, 2)$ picture with a single phase in the limit of zero deformation, $u = 0$ (phase (I) in Fig. 1).

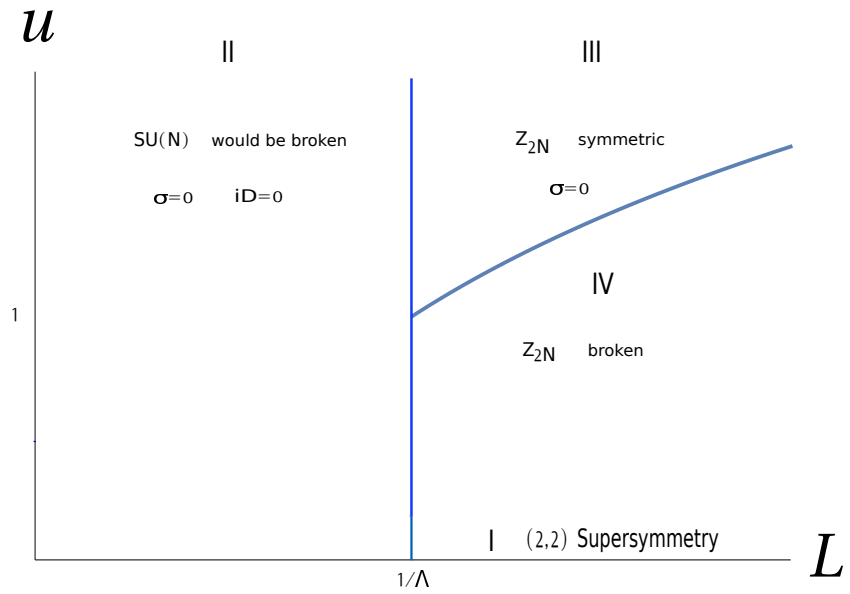

Figure 1.1: (I) $u < 1/N^2$ region corresponds to the $\mathcal{N} = (2, 2)$ solution regardless of L; (II) $u \gg 1/N^2$ and $L < 1/\Lambda$ region corresponds to the would be broken SU(N) phase (n^l fields develop VEV); (III) $L > 1/\Lambda$ and large u region represents the Z_{2N}-symmetric phase with massless fermions; (IV) $L > 1/\Lambda$ and moderate u region represents Z_{2N}-broken phase with massive bosons and fermions.

Chapter 2

Abelian and Non-Abelian Strings

2.1 Formulation of the problem

We start from the model suggested in [14]. Its overall features are similar to those of the superconducting cosmic strings [31]. The model is described by an effective Lagrangian

$$\mathcal{L} = \mathcal{L}_0 + \mathcal{L}_\chi \tag{2.1.1}$$

where

$$\begin{aligned} \mathcal{L}_0 &= -\frac{1}{4e^2} F_{\mu\nu}^2 + |\mathcal{D}^\mu \phi|^2 - V(\phi)\,, \\ \mathcal{D}_\mu \phi &= (\partial_\mu - iA_\mu)\phi\,, \\ V &= \lambda\left(|\phi|^2 - v^2\right)^2\,, \end{aligned} \tag{2.1.2}$$

and

$$\mathcal{L}_\chi = \partial_\mu \chi^i\, \partial^\mu \chi^i - U(\chi, \phi)\,, \tag{2.1.3}$$

$$U = \gamma\left[\left(-\mu^2 + |\phi|^2\right)\chi^i\chi^i + \beta\left(\chi^i\chi^i\right)^2\right], \tag{2.1.4}$$

with self-evident definitions of the fields involved, the covariant derivative, and the kinetic and potential terms. The parameters e, λ, β, μ, and v can be chosen at will, with some mild constraints (e.g. $v > \mu$) discussed in [13]. In particular, the stability of

the $\phi \neq 0$ vacuum we are interested in implies that β cannot be too small,

$$\beta \geq \frac{m_\chi^2}{m_\phi^2} \frac{1}{c(c-1)}\,, \tag{2.1.5}$$

where

$$c \equiv \frac{v^2}{\mu^2}\,, \tag{2.1.6}$$

cf. Eq. (2.1.9). The relations between the parameters in (2.1.2), (2.1.4) and a, b, c appearing below, on the one hand, and the physical parameters (the particle masses and the coefficients in front of the quartic terms ϕ^4, χ^4 and $\phi^2\chi^2$, respectively), on the other hand, are shown in Table 2.1 and (2.1.7), (2.1.9).

β	$\dfrac{\tilde{\lambda}}{\gamma}$
a	$\dfrac{m_A^2}{m_\phi^2}$
b	$\dfrac{m_\chi^2}{m_\phi^2}$
$\dfrac{v^2}{\mu^2} \equiv c$	$\left(1 - \dfrac{4\lambda}{\gamma}\dfrac{m_\chi^2}{m_\phi^2}\right)^{-1}$

Table 2.1: Parameters in (2.1.2), (2.1.4) in terms of the particle masses and the coefficients in front of the quartic terms ϕ^4, χ^4, and $\phi^2\chi^2$ (λ, $\tilde{\lambda}$, and γ, respectively).

We will assume the parameters to be chosen in such a way that the bulk model is weakly coupled and, hence, the quasiclassical approximation is applicable.

Now let us discuss some parameters and the corresponding notation. In the vacuum the complex field ϕ develops a vacuum expectation value $|\phi_{\text{vac}}| = v$ while its phase is eaten up by the Higgs mechanism. The masses of the (Higgsed) photon and the Higgs excitation are

$$m_A^2 = 2e^2v^2\,, \quad m_\phi^2 = 4\lambda v^2\,. \tag{2.1.7}$$

We will denote the ratio of the masses

$$a = m_A^2/m_\phi^2 \equiv \frac{e^2}{2\lambda}\,. \tag{2.1.8}$$

Moreover, in the vacuum the field χ^i does *not* condense. Its mass is

$$m_\chi^2 = \gamma\left(v^2 - \mu^2\right). \tag{2.1.9}$$

For what follows we will introduce two extra dimensionless parameters:

$$b = m_\chi^2/m_\phi^2 \equiv \frac{\gamma}{4\lambda}\,\frac{c-1}{c}\,, \quad c = v^2/\mu^2\,. \tag{2.1.10}$$

The first measures the ratio of the χ to ϕ masses in the bulk and, as explained in [14], has to be $b \gtrsim 1$. The second parameter is also constrained, $c > 1$. We will treat both of them as parameters of the order of unity. As for the spatial orientation, the string will be assumed to lie along the z axis. We introduce a dimensionless radius in the perpendicular $\{x, y\}$ plane,

$$\rho = m_\phi\,\sqrt{x^2 + y^2}\,. \tag{2.1.11}$$

The basis of our construction is the standard ANO string (see e.g. [32]). The ϕ field winds ensuring topological stability, which entails in turn its vanishing at the origin. This implies the following ansätze:

$$A_0 = 0\,, \quad A_i = -\varepsilon_{ij}\frac{x_j}{r^2}\left(1 - f(r)\right), \quad \phi = v\varphi(\rho)e^{i\alpha}\,, \tag{2.1.12}$$

where α is the polar angle in the perpendicular plane, and we assume for simplicity the minimal (unit) winding. The boundary conditions supplementing (2.1.12) are

$$f(\infty) = 0\,, \qquad f(0) = 1\,; \qquad \varphi(\infty) = 1\,, \quad \varphi(0) = 0\,. \tag{2.1.13}$$

In the core of such a tube the ϕ field tends to zero, see (2.1.13). The vanishing of the ϕ field results in the χ^i field destabilization in the core of the string (as follows from Eq. (2.1.4)). Hence, inside the core, the χ^i field no longer vanishes,

$$(\chi^i\chi^i)_{\rm core} \approx \frac{\mu^2}{2\beta}\,, \tag{2.1.14}$$

as will be illustrated by the graphs given below. Choosing the value of λ judiciously, we can make $\mu^2/\beta \gg m_\chi^2$, implying that the O(3) symmetry is broken in the core. The

appropriate ansatz is

$$\chi^i = \frac{\mu}{\sqrt{2\beta}}\,\chi(\rho)\begin{pmatrix}0\\0\\1\end{pmatrix}\,, \tag{2.1.15}$$

with the boundary conditions

$$\chi(\infty) = 0\,, \quad \chi(0) \approx 1\,. \tag{2.1.16}$$

Thus, we have three profile functions, f, φ, and χ, depending on ρ. Minimizing the energy functional we derive the system of equations for the profile functions

$$\begin{aligned}
\left(\frac{f'}{\rho}\right)' &= a\frac{\varphi^2 f}{\rho}\,,\\
\left(\phi'\rho\right)' &= \frac{f^2\varphi}{\rho} + \frac{\rho\varphi\left(\varphi^2-1\right)}{2} + \frac{\rho\,\varphi\,\chi^2}{2\beta}\frac{b}{c-1}\,,\\
\left(\chi'\rho\right)' &= \frac{b}{c-1}\rho\chi\left(c\varphi^2+\chi^2-1\right)\,,
\end{aligned} \tag{2.1.17}$$

where the primes denote differentiation with respect to ρ. In the numerical solution to be presented below we will assume for simplicity that

$$a = 1\,, \quad \text{i.e. } m_\phi = m_A\,. \tag{2.1.18}$$

In the absence of the χ field this would imply the Bogomol'nyi-Prasad-Sommerfield (BPS) limit [33] with the tension [1]

$$T_0 = 2\pi v^2\,. \tag{2.1.19}$$

Below we will see how the presence of the χ field changes the tension, using T_0 as a reference point.

It is obvious that the solution $\chi = 0$ and $\varphi = \varphi_0 \equiv \varphi_{\rm ANO}$ satisfies the set of equations (2.1.17). First we will show that this solution is unstable, i.e. corresponds to the maximum rather than minimum of the energy functional.

[1] Alternatively, this is the boundary between type-I and type-II superconductors.

2.2 Instability of the $\chi = 0$ solution

To prove instability we must demonstrate that for $\varphi = \varphi_0 \equiv \varphi_{\rm ANO}$ there is a negative mode in χ, in much the same way as in [31]. To this end it is sufficient to examine the energy functional in the quadratic in χ approximation,

$$\mathcal{E}_\chi = \frac{\mu^2}{2\beta}\, L \int dx\, dy \left\{ \chi \left[-\Delta + \gamma\mu^2 \left(-1 + \frac{v^2}{\mu^2}\varphi_0^2 \right) \right] \chi \right\}, \tag{2.2.1}$$

where L is the string length (tending to infinity), and find the lowest eigenvalue of

$$\left[-\Delta + \gamma\mu^2 \left(-1 + \frac{v^2}{\mu^2}\varphi_0^2 \right) \right] \chi = E\chi\,. \tag{2.2.2}$$

One can view (2.2.2) as a two-dimensional Schrödinger equation. Given that the ground state is spherically symmetric and introducing

$$\psi(\rho) = \chi\sqrt{\rho}\,, \tag{2.2.3}$$

one can rewrite (2.2.2) as

$$-\psi'' + \left(b\,\frac{c\varphi_0^2 - 1}{c-1} - \frac{1}{4\rho^2} \right) \psi = \epsilon\psi\,, \qquad \epsilon = \frac{E}{m_\phi^2}\,, \tag{2.2.4}$$

where prime denotes differentiation over ρ. Numerical solution at $c = 1.25$ yields

$$\epsilon = \begin{cases} -1.479 \ \text{ at } \ b = 1\,, \\ -4.19 \ \text{ at } \ b = 2\,. \end{cases} \tag{2.2.5}$$

2.3 $\chi \neq 0$ solution

To find the asymptotic behavior of the profile functions at $\rho \to \infty$ one can linearize these equations in this limit,

$$f \sim \sqrt{\rho}\, e^{-\rho}\,, \quad (1-\varphi) \sim \frac{1}{\sqrt{\rho}}\, e^{-\rho}\,, \quad \chi \sim \frac{1}{\sqrt{\rho}}\, e^{-\sqrt{b}\rho}\,. \tag{2.3.1}$$

We integrated Eqs. (2.1.17) numerically for a number of points in the parameter space $\{b, c, \beta\}$ keeping $a = 1$. Then the parameter λ appears only as an overall factor, with the analytically known dependence. Representative plots are given in Fig. (2.1, 2.2).

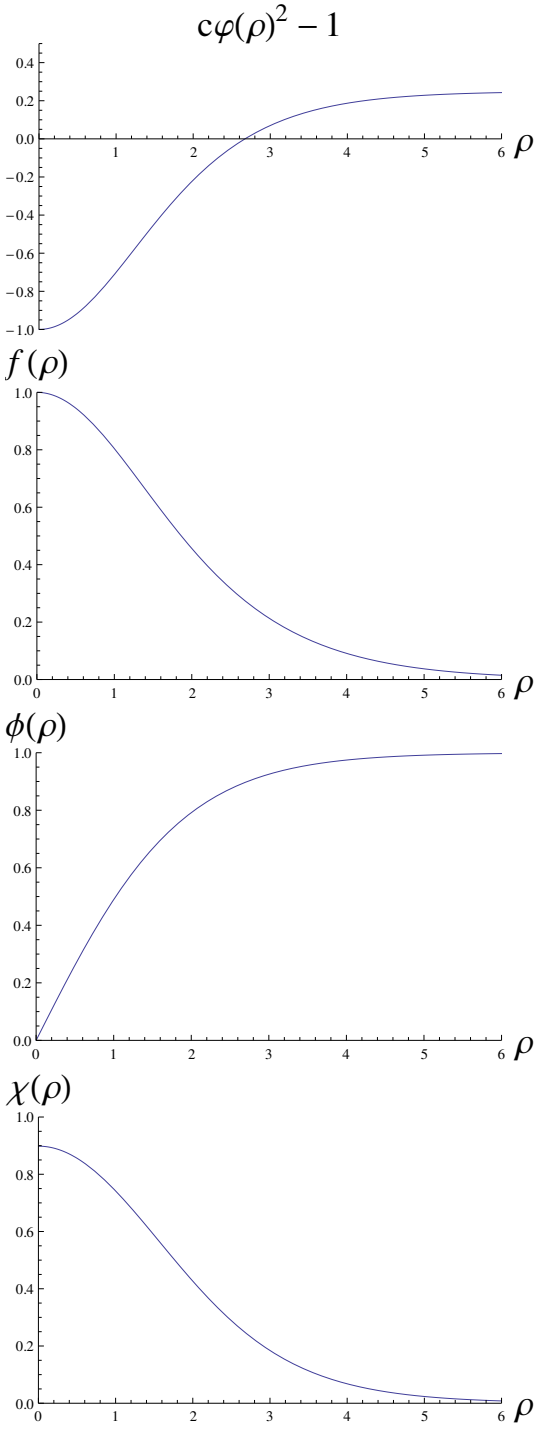

Figure 2.1: $b = 1$, $c = 1.25$, $\beta = 8$

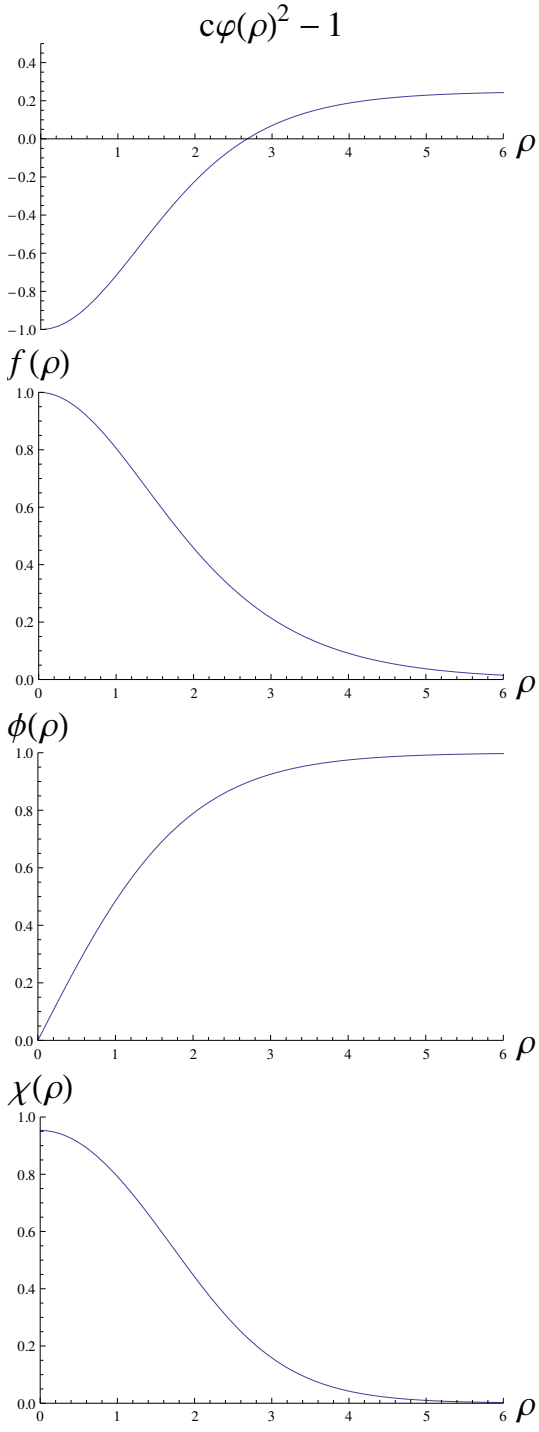

Figure 2.2: $b = 2$, $c = 1.25$, $\beta = 16$

The first plot at the very top is given to show the domain of ρ in which an "effective" m^2 for the χ field is negative forcing χ^i to condense in the core. This is the domain of negative χ^i contribution to the potential energy. Then the three profile functions are presented: $f(\rho)$, $\varphi(\rho)$, and $\chi(\rho)$ (from top to bottom). In terms of the physical parameters, Figure (2.1) corresponds to $m_\chi^2 = m_\phi^2$ and $\tilde{\lambda} = 160\lambda$ while Figure (2.2) corresponds to $m_\chi^2 = 2m_\phi^2$ and $\tilde{\lambda} = 640\lambda$.

These plots demonstrate that $\chi(0)$ is indeed close to unity. In scanning the parameter space we observe that (i) increasing the parameter b (i.e. the χ mass) increases both the width of the domain where the "effective" m^2 for the χ field is negative and the value of $\chi(0)$, but decreases the tension of the string; (ii) increasing the parameter c (i.e. decreasing μ) acts in the opposite direction; (iii) increasing the parameter β acts in the same way as increasing c but with a weaker impact.

2.4 The world-sheet theory without spin-orbit term

Now let us introduce moduli. Two translational moduli are obvious. Since they are well studied we will not dwell on this part. Of interest are the rotational moduli. Given the nontrivial solution (2.1.15) we can immediately generate a family of solutions which go through the system of equations (2.1.17), namely,

$$\chi^i = \frac{\mu}{\sqrt{2\beta}}\,\chi(\rho)\,S^i\,, \tag{2.4.1}$$

where the moduli S^i are constrained ($i = 1, 2, 3$),

$$S^i\,S^i = 1\,, \tag{2.4.2}$$

therefore, in fact, we have two moduli, as was expected. To derive the theory on the string world sheet we, as usual, introduce t, z dependence converting the S^i moduli into the moduli fields $S^i(t, z)$, and

$$\chi^i = \frac{\mu}{\sqrt{2\beta}}\,\chi(\rho)\,S^i(t, z)\,. \tag{2.4.3}$$

Substituting this in the Lagrangian (3) and (4) we obtain the low-energy effective action

$$S = \frac{1}{2g^2}\int dt\,dz\,\left(\partial_k S^i\right)^2\,, \quad k = t, z. \tag{2.4.4}$$

where

$$\frac{1}{2g^2} = \frac{1}{8c\beta\lambda}\int_0^\infty 2\pi\rho\,\chi^2(\rho)\,d\rho\,. \tag{2.4.5}$$

One can rewrite this as

$$\frac{g^2}{2\pi} = \lambda\,\frac{\beta}{\pi^2}\,\frac{c}{I_1}\,, \tag{2.4.6}$$

where

$$I_1 = \int_0^\infty \rho\,\chi^2(\rho)\,d\rho\,. \tag{2.4.7}$$

For the parameters we used in Figs. (2.1, 2.2) we obtain

$$I_1 \approx 1.107 \ \text{(for Fig. 2.1)}, \qquad I_1 \approx 1.18 \ \text{(for Fig. 2.2)}\,, \tag{2.4.8}$$

and, correspondingly,

$$\frac{g^2}{2\pi} \approx 0.915\,\lambda \ \text{(for Fig. 2.1)}\,, \qquad \frac{g^2}{2\pi} \approx 1.717\,\lambda \ \text{(for Fig. 2.2)}\,. \tag{2.4.9}$$

2.5 Spin-orbit interaction

The "two-component" ϕ-χ string solution presented above spontaneously breaks two translational symmetries, in the perpendicular x, y plane, and O(3) rotations. The latter are spontaneously broken by the string orientation along the z axis (more exactly, O(3)→O(2)), and by the orientation of the spin field χ^i inside the core of the flux tube introduced through S^i.

Now, we deform Eq. (2.1.3) by adding a spin-orbit interaction [15],

$$\mathcal{L}_\chi = \partial_\mu\chi^i\,\partial^\mu\chi^i - \varepsilon(\partial_i\chi^i)^2 - U(\chi,\phi)\,, \tag{2.5.1}$$

where ε is to be treated as a perturbation parameter.

If $\varepsilon = 0$ (i.e. Eq. (2.1.3) is valid) the breaking O(3)→O(2) produces no extra zero modes (other than translational) in the ϕ-A_μ sector [16, 17]. Due to the fact that $\chi \neq 0$ in the core, we obtain two extra moduli S^i on the world sheet. This is due to the fact that at $\varepsilon = 0$ the rotational O(3) symmetry is enhanced [13, 15] because of the O(3) rotations of the "spin" field χ^i, independent of the coordinate spacial rotations.

What happens at $\varepsilon \neq 0$, see Eq. (2.5.1)? If ε is small, to the leading order in this parameter, we can determine the effective world-sheet action using the solution

found above at $\varepsilon = 0$. Two distinct O(3) rotations mentioned above become entangled: O(3)×O(3) is no longer the exact symmetry of the model, but, rather, an approximate symmetry. The low-energy effective action on the string world sheet takes the form

$$\begin{aligned} S &= \int dt\, dz \left(\mathcal{L}_{\mathrm{O}(3)} + \mathcal{L}_{x_\perp} \right), \\ \mathcal{L}_{\mathrm{O}(3)} &= \left\{ \frac{1}{2g^2} \left[\left(\partial_k S^i\right)^2 - \varepsilon \left(\partial_z S^3\right)^2 \right] \right\} - M^2 \left(1 - (S^3)^2\right), \qquad (2.5.2) \\ \mathcal{L}_{x_\perp} &= \frac{T}{2} \left(\partial_k \vec{x}_\perp\right)^2 - M^2 (S^3)^2 \left(\partial_z \vec{x}_\perp\right)^2 \\ &+ 2M^2 \left(S^3\right) \left(S^1 \partial_z x_{1\perp} + S^2 \partial_z x_{2\perp} \right), \qquad (2.5.3) \end{aligned}$$

where $\vec{x}_\perp = \{x(t,z),\, y(t,z)\}$ are the translational moduli fields, and T is the string tension. The mass term M^2 is

$$M^2 = \varepsilon\, v^2\, \frac{\pi I_2}{2c\beta}, \qquad (2.5.4)$$

where

$$I_2 = \int_0^\infty \rho \left(\chi'(\rho)\right)^2 d\rho\,. \qquad (2.5.5)$$

For the values of parameters used in Figs. 1, 2 we obtain

$$I_2 \approx 0.378 \;\; \text{(for Fig. 1)}, \qquad I_2 \approx 0.467 \;\; \text{(for Fig. 2)}\,. \qquad (2.5.6)$$

As for the tension T we have

$$\frac{T}{T_0} \approx 0.963 \;\; \text{(for Fig. 1)}\,, \qquad \frac{T}{T_0} \approx 0.953 \;\; \text{(for Fig. 2)}\,. \qquad (2.5.7)$$

The impact of the χ^i field on the string tension is rather small and negative. The positive contribution of its kinetic energy is compensated by the negative potential energy, see Figs. (2.1, 2.2). This was expected given the result of Sec. 2.2.

Moreover, it is seen that

$$\frac{M^2}{T} \sim \frac{\varepsilon}{\beta}$$

and is small for sufficiently small ratio ε/β. This justifies the above calculation.

2.6 Degeneracy between Abelian and Non-Abelian Strings

In the previous sections we found a solution for Abelian and non-Abelian strings. For the chosen parameters the solution corresponding to the Abelian string was unstable. A natural question arises as to whether the ANO (i.e. Abelian) and non-Abelian strings can coexist in one and the same model, both being locally stable, and if yes, whether their tensions can be degenerate. The exact answer to the second question can be given only in supersymmetric models provided that both strings are BPS-saturated [33], with one and the same central charge.

Deferring this task for the future here we will explore a model described in section 2.1 to find whether or not (classically) degenerate Abelian and non-Abelian strings are simultaneously supported in this model for at least some values of parameters. We will analyze the parameter space to find examples of degenerate strings which are locally stable, i.e there are no negative modes in the string background.

We mainly follow the sections (2.2, 2.3) to (numerically) construct profile functions with zero and non-zero values of the triplet field χ, i.e. Abelian vs. non-Abelian. To justify the quasiclassical approximation we assume weak coupling in the bulk. First, to normalize our calculation, we determine the profile functions corresponding to the Abrikosov-Nielsen-Olesen string and find its tension. Next, we find the string solution with non-zero χ. We show that with the appropriate choice of the parameters the two strings are degenerate in tension at the classical level (within the accuracy of our numerical calculations). We also investigate stability of the strings.

2.6.1 The $\chi = 0$ solution

First we consider $\chi = 0$ and $\varphi = \varphi_0 \equiv \varphi_{\rm ANO}$. We follow Witten [31] to investigate the stability of the solution with regards to small χ fluctuations. To this end we write down a (linearized) equation for the χ modes around the ANO solution. The mode equation takes the form

$$-\psi'' + \left(b\,\frac{c\varphi_0^2 - 1}{c-1} - \frac{1}{4\rho^2} \right) \psi = \epsilon\psi\,, \qquad \psi(\rho) \equiv \chi\sqrt{\rho}\,. \tag{2.6.1}$$

Foe two representative values of parameters the numerical solution yields

$$\epsilon = \begin{cases} 0.041 \ \text{ at } \ b = 0.0987\,, \ c = 1.17\,, \\ \\ 0.234 \ \text{ at } \ b = 1.871\,, \ c = 2\,. \end{cases} \tag{2.6.2}$$

The positivity of ϵ implies the stability of the $\chi = 0$ solution. The tension of the string was found to be

$$\frac{T_0}{2\pi v^2} = 1 - O(10^{-7})\,. \tag{2.6.3}$$

The second number on the right-hand side of Eq. (2.6.3) represents the accuracy of our numerical computations.

2.6.2 The $\chi \neq 0$ solution

Now we will demonstrate that although the above ANO solution is locally stable, the model at hand supports a solution with non-Abelian moduli, i.e. with $\chi \neq 0$.

In the case of $\chi \neq 0$ one can find the asymptotic behavior of the profile functions at $\rho \to \infty$ by linearizing these equations in this limit,

$$f \sim \sqrt{\rho}\, e^{-\rho}\,, \quad (1-\varphi) \sim \frac{1}{\sqrt{\rho}}\, e^{-\rho}\,, \quad \chi \sim \frac{1}{\sqrt{\rho}}\, e^{-\sqrt{b}\rho}\,. \tag{2.6.4}$$

Then we integrated Eqs. (2.1.17) numerically, keeping $a = 1$ and varying parameters $\{b, c, \beta\}$. The plots of the profile functions are shown in Figs. (2.3, 2.4). One can note a rather low value of the χ field in the core. In order for the χ field not to be smeared by quantum fluctuations we must additionally impose a constraint on the parameters

$$\tilde{\lambda} \ll \frac{\chi^2(0)}{2(c-1)}\,. \tag{2.6.5}$$

Fortunately, this is always possible since the value of $\tilde{\lambda}$ is in our hands. The origin of Eq. (2.6.5) is as follows. The value of the field χ in the core of the string should be much larger than the mass, otherwise quasiclassical treatment is not applicable (the condensate of the field should contain many quanta). The mass of the χ field is given in Eq. (2.1.9). The normalization of the field given in Eq. (2.1.14) should be modified, taking into account the results of our numerical calculation for $\chi(0)$. Thus, the above ratio is expressed as follows

$$\frac{\chi^2_{\rm core}}{m^2_\chi} = \frac{\mu^2}{2\beta}\, \chi^2(0)\, \frac{1}{\gamma(v^2 - \mu^2)} \gg 1\,, \tag{2.6.6}$$

which reduces to Eq. (2.6.5).

Similarly to the consideration in Sec. 2.6.1, we determine the lowest eigenvalue of the equation

$$-\psi'' + \left[\frac{b}{c-1}\left(c\varphi_1^2 - 1 + 3\chi_1^2\right) - \frac{1}{4\rho^2}\right]\psi = \epsilon\psi\,, \tag{2.6.7}$$

where φ_1, and χ_1 are the solutions presented in Fig. 1. This is necessary to check the stability of $\chi \neq 0$ solution with regards to local variations of χ. The results of numerical calculations yield

$$\epsilon = \begin{cases} 0.042 \;\text{ at }\; b = 0.0987\,,\; c = 1.17\,, \\ \\ 0.235 \;\text{ at }\; b = 1.871\,,\; c = 2\,. \end{cases} \tag{2.6.8}$$

We determined the tension of the non-Abelian string,

$$\frac{T_0}{2\pi v^2} = 1 - O(10^{-7}) \tag{2.6.9}$$

which must be compared with Eq. (2.6.3). We observe the degeneracy of the two strings (with $\chi = 0$ and $\chi \neq 0$).

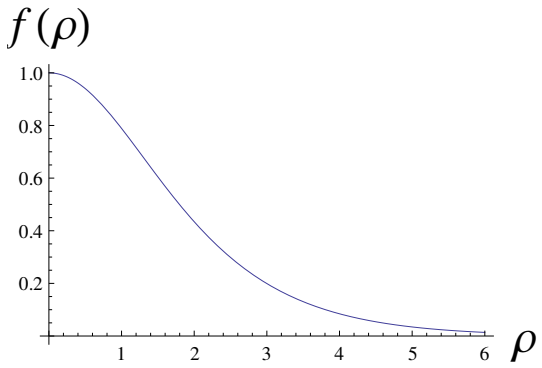

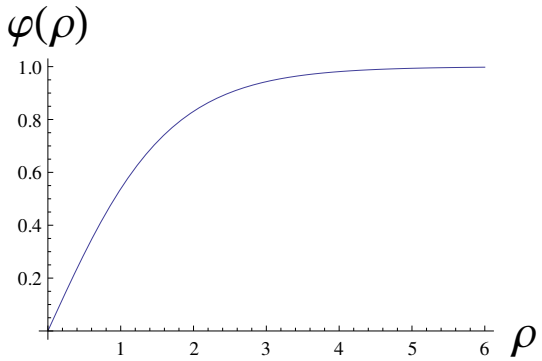

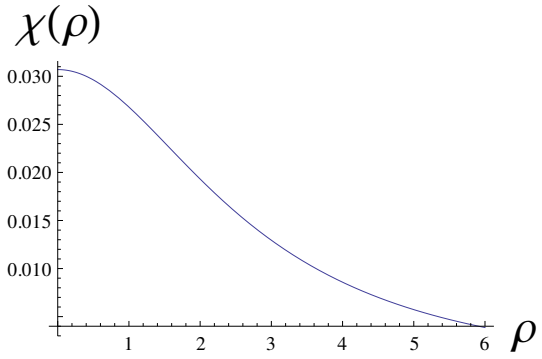

Figure 2.3: $b = 0.0987$, $c = 1.17$, $\beta = 1.1\beta_*$

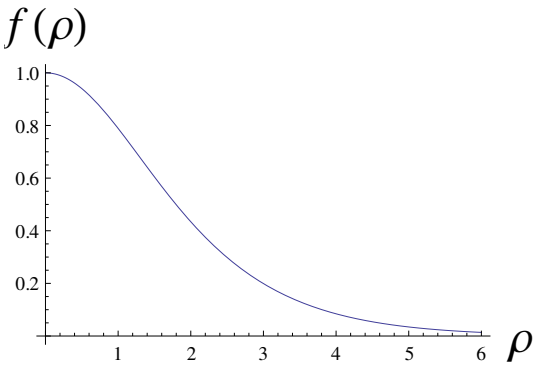

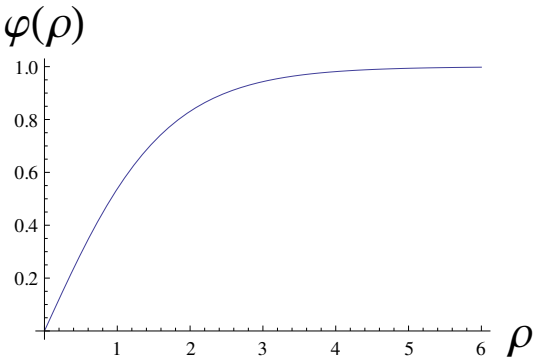

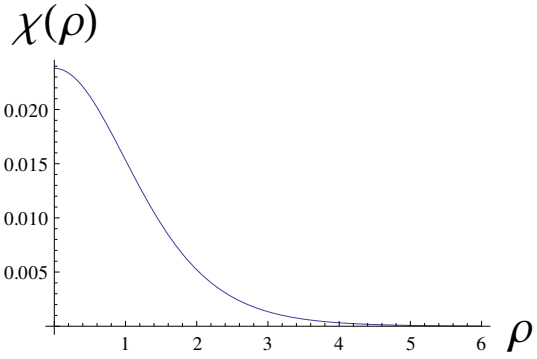

Figure 2.4: $b = 1.871$, $c = 2$, $\beta = 1.1\beta_*$

Chapter 3

Non-Abelian String of a Finite Length

3.1 Non-supersymmetric non-Abelian strings

In this section we briefly review the simplest four-dimensional non-supersymmetric model supporting non-Abelian strings [18], give a topological argument for their stability and outline the effective low-energy theory on the world-sheet.

The model suggested in [18] is a bosonic part of $\mathcal{N} = 2$ supersymmetric QCD, see [10] for a review. The gauge group of the theory is $SU(N) \times U(1)$. The matter sector of the model consists of $N_f = N$ flavors of complex scalar fields (squarks) charged with respect to $U(1)$, each in the fundamental representation of $SU(N)$. The action of the model is

$$\begin{aligned} S &= \int d^4x \Big[-\frac{1}{4g_2^2} \left(F^a_{\mu\nu}\right)^2 - \frac{1}{4g_1^2} \left(F_{\mu\nu}\right)^2 \\ &+ |\nabla^\mu \varphi^A|^2 + \frac{g_2^2}{2} \left(\bar{\varphi}_A T^a \varphi^A\right)^2 + \frac{g_1^2}{8} \left(|\varphi^A|^2 - N\xi\right)^2 \Big] , \end{aligned} \tag{3.1.1}$$

where T^a are the generators of $SU(N)$, the covariant derivative is defined as

$$\nabla_\mu = \partial_\mu - \frac{i}{2} A_\mu - i T^a A^a_\mu ,$$

A_μ and A^a_μ denote the $U(1)$ and $SU(N)$ gauge fields respectively, and the corresponding coupling constants are g_1 and g_2. The scalar fields φ^{kA} have the color index $k = 1, ..., N$ and the flavor index $A = 1, ..., N$. Thus, φ^{kA} can be viewed as an $N \times N$ matrix. The $U(1)$ charges of φ^{kA} are $1/2$.

Let us examine the potential of the theory (3.1.1) in more detail. It consists of two non-negative terms and consequently the minimum of the potential is reached when both terms vanish. The last term proportional to g_1^2 forces φ^A to develop a vacuum expectation value. One can choose φ^{kA} to be proportional to the unit matrix, namely,

$$\varphi_{vac} = \sqrt{\xi}\ \mathrm{diag}\ (1, 1, ..., 1), \tag{3.1.2}$$

where we use $N \times N$ matrix notation for φ^{kA}. Then the last but one term vanishes automatically.

The above vacuum field spontaneously breaks both the gauge and flavor $SU(N)$ groups. However, it is invariant under the action of combined color-flavor global $SU(N)_{C+F}$. Therefore, symmetry breaking pattern is

$$U(N)_{\text{gauge}} \times SU(N)_{\text{flavor}} \to SU(N)_{C+F}\,.$$

This setup was suggested in [34] and became known later as the color-flavor locking.

The topological stability of non-Abelian strings in this model is due to the fact that $\pi_1(SU(N) \times U(1)/Z_N) \neq 0$. One combines the Z_N center of $SU(N)$ with elements $e^{2\pi ik/N}$ of $U(1)$ to get windings in both groups simultaneously.

The string solution [18] breaks the global symmetry of the vacuum as follows:

$$SU(N)_{C+F} \to SU(N-1) \times U(1)\,. \tag{3.1.3}$$

As a result the orientational zero modes appear, making the vortex non-Abelian. As is clear from the symmetry breaking pattern of Eq. (3.1.3) the orientational moduli belong to the quotient

$$\frac{SU(N)}{SU(N-1) \times U(1)} = CP(N-1)\,. \tag{3.1.4}$$

Thus, the low-energy effective theory on the string world-sheet is described by the $CP(N-1)$ model. The action of the model was derived in [18]; it can be written as

$$S^{(1+1)} = \int d^2x \left[\frac{T_{\text{cl}}}{2} (\partial_k z^i)^2 + r\, |\nabla_k\, n^l|^2 \right], \tag{3.1.5}$$

where

$$T_{\rm cl} = 2\pi\xi \tag{3.1.6}$$

is the classical tension of the string, z^i are two translational moduli in the perpendicular plane, n^l, $l = 1, ..., N$ are N complex fields subject to the constraint

$$|n^l|^2 = 1\,, \tag{3.1.7}$$

and r is defined below.

The covariant derivative is

$$\nabla_k = \partial_k - iA_k \tag{3.1.8}$$

and $k = (1, 2)$ labels the world-sheet coordinates. The relation between two-dimensional coupling r and a four dimensional coupling g_2 at the scale $\sqrt{\xi}$ is given by

$$r = \frac{4\pi}{g_2^2}. \tag{3.1.9}$$

The field A_k enters without kinetic term and is auxiliary. It can be eliminated by virtue of equations of motion and is introduced to make the $U(1)$ gauge invariance of the model explicit.

Let us count the number of degrees of freedom. The complex scalar fields give $2N$ real degrees of freedom, of which one is eliminated due to the constraint (3.1.7) and another one due to $U(1)$ gauge invariance. Thus, the total number of degrees of freedom is $2(N-1)$ which is precisely the number of degrees of freedom in the $CP(N-1)$ model.

To conclude this section we note that formation of non-Abelian strings leads to confinement of monopoles in the bulk theory. In fact, in the U(N) gauge theories strings are stable and cannot be broken. Therefore, confined monopoles are presented by junctions of two degenerate non-Abelian strings of different kinds, see review [10] for details. In the effective world-sheet theory on the string these confined monopoles are seen as CP($N-1$) kinks interpolating between distinct vacua.

3.2 $CP(N-1)$ model at zero temperature

At large N the model was solved [26] in the $1/N$ approximation. Let us outline how this is done. The Lagrangian $\mathcal{L}$ of the $CP(N-1)$ model in the gauged formulation in

the Euclidean space-time can be written as

$$\mathcal{L} = |\nabla_k n^l| + \omega \left(|n^l|^2 - r \right) , \tag{3.2.1}$$

where we rescale the n^l fields. In addition, we introduce a parameter ω to enforce the constraint. Moreover, we replace the coupling r with the 't Hooft coupling constant λ,

$$\lambda = \frac{N}{r} ; \tag{3.2.2}$$

λ does not scale with N.

Since the n^l fields appear quadratically in the action (3.2.1) we can perform the Gaussian integration over them resulting in the equation for the effective potential V,

$$e^{-\hat{T}V} = \int d\omega \, dA_k \det{}^{-N} \left(-(\partial_k - iA_k)^2 + \omega \right) \exp\left(\frac{N}{\lambda} \int d^2x \, \omega \right) , \tag{3.2.3}$$

where $\hat{T}$ stands for the (asymptotically infinite) Euclidean time.

Since integration over ω and A_k cannot be done exactly we use a stationary phase approximation. Due to the Lorentz invariance we search for a point such that $A_k = 0$ and $\omega = \text{const}$. To find this stationary point we vary the Eq. (3.2.3) with respect to ω. The resulting equation is

$$\lambda \int \frac{d^2k}{(2\pi)^2} \frac{1}{k^2 + \omega} = 1 . \tag{3.2.4}$$

Rewriting the bare coupling constant λ in terms of the scale Λ_{CP} of the CP$(N-1)$ model

$$\frac{4\pi}{\lambda} = \ln \frac{M_{\text{uv}}^2}{\Lambda_{\text{CP}}^2} , \tag{3.2.5}$$

where M_{uv} is the ultra-violet cutoff, we finally find that

$$\omega = \Lambda_{\text{CP}}^2 . \tag{3.2.6}$$

Thus, the vacuum value of ω does not vanish. Looking at Eq. (3.2.1) one can see that a positive value of ω means that a mass for the fields n^l is dynamically generated.

To determine the spectrum of the theory one has to expand the effective action Eq. (3.2.1) around the saddle point and consider field fluctuations in the quadratic approximation. Linear terms vanish. Terms that are cubic and higher are suppressed by powers of $1/\sqrt{N}$. Two Feynman diagrams in Fig. 3.1 give rise to the kinetic term for the U(1) gauge field.

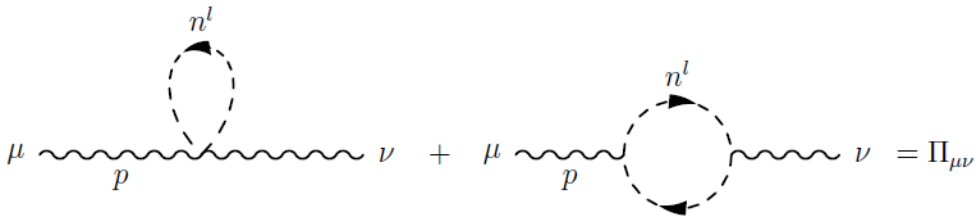

Figure 3.1: Feynman diagrams contributing to kinetic term of photon field

Gauge invariance requires the answer to be

$$\Pi_{\mu\nu} = \Pi(p^2)\left(p^2 g_{\mu\nu} - p_\mu p_\nu\right) . \tag{3.2.7}$$

The meaning of Eq. (3.2.7) is simple. It represents the kinetic energy of the gauge field written in momentum space. Thus, what was introduced as an auxiliary field becomes a propagating field. Calculation in Appendix B reproduces Witten's result [26], $\Pi(0) = N/12\pi\Lambda_{\rm CP}^2$, which is interpreted as the inverse of the $U(1)$ charge squared of the n^l fields.

Massless photon in two dimensions produces the Coulomb potential between two charges at separation R,

$$V(R) = \frac{12\pi\Lambda^2}{N} R\,, \tag{3.2.8}$$

leading to a linear confinement of the $\bar{n}n$ pairs. Thus, the spectrum of the theory contains $\bar{n}n$ "mesons" rather than free n's.

It is instructive to present an alternative interpretation of this result. In [26] it was shown that n^l fields can be interpreted as kinks interpolating between different vacua. The vacuum structure of the $CP(N-1)$ model was studied in [35]. According to this work the genuine vacuum is unique. There are, however, of the order N quasivacua, which become stable in the limit $N \to \infty$, since the energy split between the neighboring quasivacua is $O(1/N)$. Thus, one can imagine the $\bar{n}$ field interpolating between the true vacuum and the first quasivacuum and the n field returning to the true vacuum as in Fig. 3.2. The linear confining potential between the kink and antikink is associated with the excess in the quasivacuum energy density compared to that in the genuine vacuum.

This two-dimensional confinement of kinks can be interpreted in terms of strings

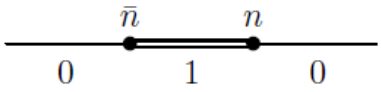

Figure 3.2: Configuration of the string with two particles on it. Zero and one represent the true vacuum and the first quasivacuum respectively.

and monopoles of the bulk theory, see [18]. The fine structure of the CP($N-1$) vacua on the non-Abelian string means that N elementary strings are split by quantum effects and have slightly different tensions. Therefore, the monopoles, in addition to the four dimensional confinement, (which ensures that they are attached to the string) acquire a two-dimensional confinement along the string. The monopole and antimonopole connected by a string with larger tension form a mesonic bound state.

Consider a monopole-antimonopole pair interpolating between strings 0 and 1, see Fig. 3.2. The energy of the excited part of the string (labeled as 1) is proportional to the distance as in Eq. (3.2.8). When it exceeds the mass of two monopoles (which is of order of $\Lambda_{\rm CP}$) then the second monopole-antimonopole pair appear breaking the excited part of the string. This gives an estimate for the typical length of the excited part of the string, $R \sim N/\Lambda_{\rm CP}$.

The above condition guarantees that there is enough energy in the "wrong string" to produce a pair of kinks. However, the probability of this process, string breaking, (which can be inferred from the false vacuum decay theory) is proportional to $\exp(-N)$, i.e. dies off exponentially at large N.

3.3 The Coulomb/confinement phase

In order to consider closed non-Abelian strings of length L we compactify the space dimension; in other words, we study CP($N-1$) model (3.2.1) on a strip of the finite length L with periodic boundary conditions.

In Euclidean formulation considering a model at finite length is equivalent to considering the model at finite temperature. The correspondence between the length of the

string and the temperature is given by

$$L = \beta\,, \tag{3.3.1}$$

where β is the inverse temperature. Thus, the limit of infinite length is the same as the limit of zero temperature.

To solve the CP($N-1$) model on a finite strip we use large-N approximation. The $CP(N-1)$ model at finite temperature in the large-N approximation was solved previously by Affleck [36], see also [37] and [38] for reviews. Although we use a different regularization, our results match those obtained in [36]. There are two important differences, however. The first one is related to the interpretation of the photon mass. In [36] the emergence of the photon mass is interpreted as a phase transition into the deconfinement phase already at $L = \infty$. We give a different interpretation of the photon mass (see Sec. 3.3.2); we do not detect any phase transition at $L = \infty$. We interpret the large L phase ($L > 1/\Lambda_{\rm CP}$) as a Coulomb/confinement phase, much in the same way as at infinite L [26].

The second difference with Ref. [36] is that we find a phase transition at $L \sim 1/\Lambda_{\rm CP}$ into a deconfinement phase in the limit $N \to \infty$, see Sec. 3.4. This is a weak coupling phase. In this phase the global SU(N) is broken and the CP($N-1$) model does not develop a mass gap. The gauge field remains auxiliary and no Coulomb/confining potential is generated.

At large but *finite* N we expect the phase transition to become a rapid crossover. The spontaneous breaking of the global SU(N) symmetry is in a contradiction with the Coleman theorem [39], stating that there can be no massless non-sterile particles in $1+1$ dimensions. Therefore we expect that the "would be Goldstone" states of the broken phase acquire small masses suppressed in the large-N limit.

To solve the CP($N-1$) model we use the mode expansion with the periodic boundary conditions. The open string setup involves the Dirichlet boundary conditions. For example, for open string the expansion (1.0.1) is modified. It acquires L-independent terms coming from the energy associated with boundaries. Here we limit ourselves to a closed string.

3.3.1 Large-N solution

Our starting point is Eq. (3.2.1). Integrating out n^l fields, one arrives at the same Eq. (3.2.3) as in the infinite L case. However, now we take into account the gauge holonomy around the compact dimension. Following [36] we choose the gauge

$$A_1 = 0$$

and look for minima of the potential with $A_0 = \text{const}$ and $\omega = \text{const}$. The mode expansion in (3.2.3) gives for the orientational part of the string energy in (1.0.3)

$$E_{\text{orient}}(L) = \frac{N}{2\pi} \sum_{k=-\infty}^{\infty} \int_{-\infty}^{\infty} dq_1 \ln \left\{ q_1^2 + \left(\frac{2\pi k}{L} + A_0 \right)^2 + \omega \right\}. \tag{3.3.2}$$

To calculate (3.3.2) we follow [40] and use the zeta function regularization. Details of our calculation are presented in Appendix A. Here we give the final result for the string vacuum energy,

$$E_{\text{orient}}(L) = \frac{NL\omega}{4\pi} \left[1 - \ln \frac{\omega}{\Lambda_{CP}^2} - 8 \sum_{k=1}^{\infty} \frac{K_1(kL\sqrt{\omega})}{kL\sqrt{\omega}} \cos kLA_0 \right], \tag{3.3.3}$$

where K_1 is the modified Bessel function of the second kind (also known as the Macdonald function). An important feature of this expression is the appearance of a non-trivial potential for the photon field. We will dwell on this issue in the next subsection.

To find the saddle point we extremize the expression (3.3.3) with respect to ω and A_0, which results in the following equations:

$$\frac{\partial E_{\text{orient}}}{\partial A_0} = \frac{2NL\sqrt{\omega}}{\pi} \sum_{k=1}^{\infty} K_1(Lk\sqrt{\omega}) \sin LkA_0 = 0\,, \tag{3.3.4}$$

$$\log \frac{\omega}{\Lambda_{\text{CP}}^2} = 4 \sum_{k=1}^{\infty} K_0(Lk\sqrt{\omega}) \cos LkA_0\,, \tag{3.3.5}$$

where the logarithmic term in the left-hand side of Eq. (3.3.5) is the renormalized inverse coupling $1/\lambda$. The logarithmic integral over momentum is regularized in the infrared by ω.

Equation (3.3.4) yields the solution of the form $LA_0 = \pi\, l$, where $l \in \mathbb{Z}$. However, from the Eq. (3.3.3) it is clear that the solution with $LA_0 = 2\pi\, l$ lies lower in energy

than the solution with $LA_0 = (2l-1)\pi$ and is, thus, physical. We take $A_0 = 0$ as a solution of (3.3.4). Our result for the orientational string energy is shown in Fig. 3.3, where $\tilde{V} = E_{\text{orient}}/L$.

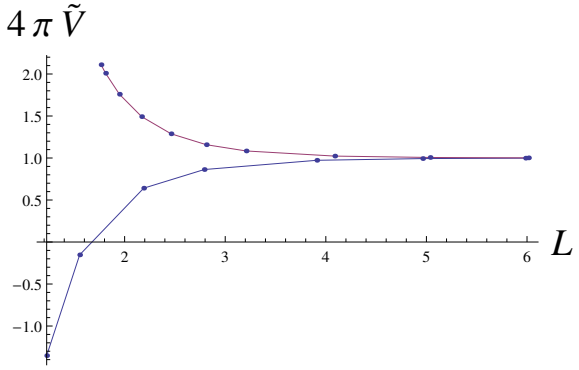

Figure 3.3: Effective potential (in units of Λ_{CP}^2) as a function of length.

Equation (3.3.5) yields a nonvanishing value of ω which we interpret – as in the case of zero temperature – as mass generation for the n^l fields. The dependence of the mass on the string length L is shown in Fig. 3.4 where we put

$$\sqrt{\omega} \equiv m\,. \tag{3.3.6}$$

One can see that the n^l field mass increases with decreasing L.

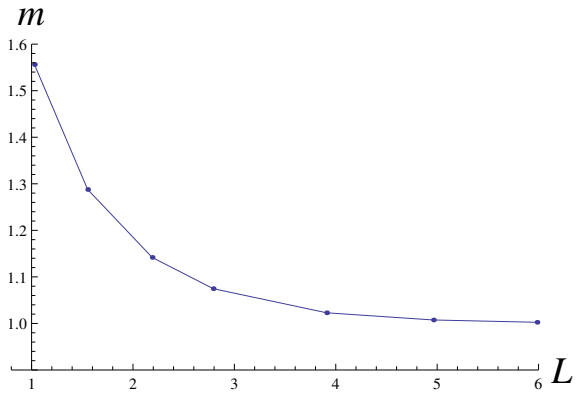

Figure 3.4: Mass (in the units of Λ) of fields n^l as a function of L.

In the limit $L \gg 1/\Lambda_{\text{CP}}$ the modified Bessel functions in (3.3.3) exhibit exponential fall-off at large L. To determine the leading non-trivial correction to the string energy

we can use the "zeroth-order" solution $\omega \approx \Lambda^2_{\rm CP}$ of the equation (3.3.5) for the vacuum expectation value (VEV) of ω. Clearly this "zeroth-order" solution coincides with the VEV of ω in the infinite volume, see (3.2.6). For the total string energy we obtain

$$E(L) = \left(2\pi\xi + \frac{N}{4\pi}\,\Lambda^2_{\rm CP}\right)\, L - \frac{\pi}{3}\,\frac{1}{L} - N\sqrt{\frac{2}{\pi}}\,\sqrt{\frac{\Lambda_{\rm CP}}{L}}\,e^{-\Lambda_{\rm CP}L} + \cdots\,. \tag{3.3.7}$$

In Eq. (3.3.7) we included the classical string tension $2\pi\xi L$, its renormalization due to vacuum fluctuations in $CP(N-1)$ (i.e. $(N/4\pi)\,\Lambda^2_{\rm CP}\,L$), and the contribution of the translational modes which give the standard Lüscher term. This result was quoted in Chapter 1, see Eq. (1.0.5).

We see that the quantum fluctuations of the orientational moduli contribute both to the renormalization of the string tension (the linear in L term in (3.3.7)) and to the function $f(\Lambda_{CP}L)$ in (1.0.3). As was expected, in the theory with a mass gap the contribution of orientational moduli to the L-dependent part of the string energy is exponentially suppressed at large L.

Let us note, that the case of an open non-Abelian string was previously considered in [41]. The results of [41] show the presence of long range $1/L$ effects coming from the orientational sector even at large L where the theory has a mass gap. We disagree with these results and believe that orientational long range forces in the large-L phase are spurious and are associated with the boundary energy somehow induced [41] by the Dirichlet boundary conditions rather than with the string itself.

3.3.2 The photon mass

The A_0-dependence in the potential (3.3.3) ensures that the gauge field acquires a mass [36]. It is quite natural to expect that the photon becomes massive at non-zero temperature. Physically this means the Debye screening.

Expanding (3.3.3) at large L we can write down an effective action for the U(1) gauge field,

$$S_{\rm gauge} = \int d^2x \left\{ \frac{1}{4e^2}\,F^2_{kl} - N\sqrt{\frac{2}{\pi}}\,\sqrt{\frac{\Lambda_{CP}}{L^3}}\,e^{-\Lambda_{\rm CP}L}\,\cos A_0 L + \cdots \right\}. \tag{3.3.8}$$

The kinetic term for the gauge field at non-zero temperature is calculated in Appendix B. To calculate the photon mass to the leading order in $\exp\left(-\Lambda_{\rm CP}L\right)$ we need

the expression for the gauge coupling e^2 in the limit $L \to \infty$, namely,

$$\frac{1}{e^2} \approx \frac{N}{12\pi\Lambda_{\rm CP}^2}, \tag{3.3.9}$$

see Sec. 3.2. Expanding (3.3.8) to the quadratic order in A_0 we arrive at

$$m_A^2 \approx 12\Lambda_{\rm CP}^2 \sqrt{2\pi\Lambda_{\rm CP} L}\, e^{-\Lambda_{\rm CP} L}\,. \tag{3.3.10}$$

for the photon mass. Note, that the non-zero photon mass at finite temperature does not break gauge invariance since Lorentz symmetry is explicitly broken, see [36].

The photon becoming massive was the reason for the claim [36] that at non-zero temperature the CP($N-1$) model is in the deconfinement phase. We give a different interpretation for this effect.

We treat the quasivacua as the strings of different tension. Kinks and antikinks interpolate between true vacuum and the first quasivacuum. The Debye screening due to a finite photon mass now can be interpreted as a breaking of the confining string between kink and antikink in the thermal medium (through picking up a kink-antikink pair from the thermal bath). Note, that unlike pair-production from the vacuum, this process is not suppressed as $\exp(-N)$.

The kink-antikink potential has the form

$$V(R) = e^2\, R\, e^{-m_A R}\,, \tag{3.3.11}$$

where R is the kink-antikink separation. It is still linear at small R, while the exponential suppression at large R can be understood as a breaking of the confining string due to creation of a kink-antikink pair from the thermal bath. Therefore, we still interpret the large L phase as a Coulomb/confinement phase.

A similar question can be addressed in QCD. Do we have confinement of quarks in QCD? We believe that the answer is positive. However, the confining string can be broken by quark-antiquark production. We suggest a similar interpretation for the CP($N-1$) model at non-zero temperature.

If L is very large (very low temperatures) the thermal string breaking can be ignored, however once L reduces below $\log N/\Lambda_{\rm CP}$ the thermal breaking becomes operative.

3.3.3 Small length limit

As was already mentioned, we will show in the next section that once L decreases below $1/\Lambda_{CP}$ our CP($N-1$) model undergoes a phase transition into the deconfinement phase. To prove this we calculate the vacuum energy in the deconfinement phase in the next section and show that it lies below that in the Coulomb/confinement phase.

In order to make this comparison we will examine Eqs. (3.3.3) and (3.3.5) in the low-L limit. These expressions determine the vacuum energy and the ω expectation value in the Coulomb/confinement phase.

Assuming that $L^2\omega \ll 1$ we can use the following approximation for the sum of the modified Bessel functions (see Eq. (8.526) in [42])

$$\sum_{n=1}^{\infty} K_0(ny) \approx \frac{\pi}{2y} + \frac{1}{2}\ln\frac{y}{4\pi} + \frac{\gamma}{2} + O(y^2)\,, \tag{3.3.12}$$

where $\gamma \approx 0.577$ is the Euler-Mascheroni constant. Consequently, we get from (3.3.5)

$$\ln\frac{\sqrt{\omega}}{\Lambda_{CP}} = 2\left[\frac{\pi}{2L\sqrt{\omega}} + \frac{1}{2}\ln\frac{L\sqrt{\omega}}{4\pi} + \frac{\gamma}{2}\right]\,, \tag{3.3.13}$$

or approximately

$$\ln\frac{1}{\Lambda_{CP}L} = \frac{\pi}{L\sqrt{\omega}}. \tag{3.3.14}$$

Now the logarithmic integral which determines the renormalized inverse coupling $1/\lambda$ is regularized in the infrared by $1/L$ rather than by $\sqrt{\omega}$ (which is the case in the large-L limit). This gives us the ω expectation value,

$$\sqrt{\omega} = \frac{\pi}{L}\,\frac{1}{\ln\left(1/\Lambda_{\rm CP}L\right)} + \cdots\,. \tag{3.3.15}$$

Equation (3.3.15) justifies our approximation $L^2\omega \ll 1$ at $L \ll 1/\Lambda_{CP}$. Note also that at $L \ll 1/\Lambda_{CP}$ the coupling constant is small – it is frozen at the scale $1/L$ (the logarithm in the left-hand side of (3.3.14) is large), so the theory is at weak coupling.

To find the orientational energy in this limit we need to find an approximate expression for the sum of the modified Bessel functions that appears in (3.3.3),

$$S_E = \frac{2L\sqrt{\omega}}{L\pi}\sum_{k=1}^{\infty}\frac{K_1(kL\sqrt{\omega})}{k}\,. \tag{3.3.16}$$

Derivative of the modified Bessel functions satisfies the following relation (see Eq. (9.6.28) in [43]):

$$K_1'(x) = -K_0(x) - \frac{K_1(x)}{x}\,. \tag{3.3.17}$$

Let us introduce a notation,

$$S_1(x) = \sum_{k=1}^{\infty} \frac{K_1(kx)}{k}\,. \tag{3.3.18}$$

Then

$$(xS_1(x))' = -x\sum_{k=1}^{\infty} K_0(kx) \overset{(3.3.12)}{\approx} -\frac{\pi}{2} - \frac{x}{2}\ln\frac{x}{4\pi} - \frac{x\gamma}{2} + O(x^3)\,. \tag{3.3.19}$$

Integrating this expression one finds

$$xS_1(x) \approx -\frac{x\pi}{2} - \frac{x^2}{4}\ln\frac{x}{4\pi} - \frac{x^2}{8}(2\gamma - 1) + \text{const} + O(x^4) \tag{3.3.20}$$

The behavior of the modified Bessel function at small values of the argument is given by (see Eq. (9.6.9) in [43])

$$K_1(x) \sim \frac{1}{x}\,. \tag{3.3.21}$$

Thus, the sum $S_1(x)$ can be approximated as follows:

$$S_1(x) \approx \sum_{k=1}^{\infty} \frac{1}{xk^2} = \frac{\pi^2}{6x}\,. \tag{3.3.22}$$

Hence the constant appears to be $\pi^2/6$. Now we are ready to present the approximate expression we seek for,

$$S_E = \frac{2}{L\pi} L\sqrt{\omega} S_1(L\sqrt{\omega}) \approx \frac{\pi}{3L} - \sqrt{\omega} - \frac{L\omega}{2\pi}\ln\frac{L\sqrt{\omega}}{4\pi} - \frac{L\omega}{4\pi}(2\gamma - 1)\,. \tag{3.3.23}$$

With this approximation we arrive at the orientational energy

$$E_{\text{orient}}(L) = -\frac{\pi}{3}\frac{N}{L} + N\sqrt{\omega} - \frac{N}{2\pi}\omega L \ln\frac{1}{\Lambda_{CP}L} + \cdots \tag{3.3.24}$$

Substituting here the VEV of ω, see (3.3.15), we get

$$E_{\text{orient}}(L) = -\frac{\pi}{3}\frac{N}{L} + \frac{\pi}{2}\frac{N}{L}\frac{1}{\ln(1/\Lambda_{CP}L)} + \cdots\,. \tag{3.3.25}$$

The first term here is the Lüscher term proportional to the number of orientational degrees of freedom $2(N-1) \approx 2N$ (in the large N limit). It gets corrected by an infinite series of powers of inverse logarithms $\ln(1/\Lambda_{CP}L)$, if we naively extend the Coulomb/confinement phase into the region of small L. We will show in the next section that in fact the theory undergoes a phase transition into a different phase, with a lower energy.

3.4 Deconfinement phase

Classically CP($N-1$) model has $2(N-1)$ massless states which can be viewed as Goldstone states of the broken SU(N) symmetry. Indeed, classically the vector n^l satisfies a fixed length condition, $|n|^2 = r$, see (3.2.1). Thus classically n^l acquires a VEV breaking SU(N) symmetry.

However, as was shown above, in the strong coupling large L domain the spontaneous symmetry breaking does not occur, in much the same way as in the infinite-L limit, see [26]. At strong coupling the vector n^l is smeared all over the vacuum manifold due to strong quantum fluctuations. The theory has a mass gap, moreover the number of the massive n-fields becomes $2N$. Effectively the classical constraint $|n|^2 = r$ is lifted, see [26].

At small L the theory enters a weak coupling regime so we expect occurrence of the classical picture in the limit $N \to \infty$. To study this possibility we assume that one component of the field n^l, say $n_0 \equiv n$ can develop a VEV. Then we integrate over all other components of n^l (l=1,2,...) keeping the fields n and ω as a background. Note, that a similar method was used in [44] for studying phase transitions in the CP($N-1$) model with twisted masses.

Now, instead of (3.3.24), we get

$$E_{\rm orient}(L) = \omega L\,|n|^2 - \frac{\pi}{3}\,\frac{N}{L} - \frac{N}{2\pi}\,\omega L\,\ln\frac{1}{\Lambda_{\rm CP}L} + \cdots\,, \tag{3.4.1}$$

where the ellipses stand for higher terms in $L^2\omega$. Note, that here we drop the contribution associated with the integration over the constant n (the second term in (3.3.24)) because we introduce n_0 as a constant background field (in other words, we drop the term with $k=0$ in (3.3.2)).

Minimizing over ω and n we arrive at the equations

$$\begin{aligned} |n|^2 &= \frac{N}{2\pi}\,\ln\frac{1}{\Lambda_{CP}L}+\ldots, \\ \omega\, n &= 0\,. \end{aligned} \tag{3.4.2}$$

The solution to these equations with nonzero n_0 read

$$|n|^2=\frac{N}{2\pi}\,\ln\frac{1}{\Lambda_{CP}L}, \qquad \omega=0\,. \tag{3.4.3}$$

We see that the mass gap ω is not generated. Substituting this in (3.4.1) we get that the orientational energy reduces just to the Lüscher term, namely

$$E_{\rm orient}(L)=-\frac{\pi}{3}\,\frac{N}{L}. \tag{3.4.4}$$

This energy is lower than the one in (3.3.25). Therefore, we conclude that at $L\sim 1/\Lambda_{CP}$ the theory undergoes a phase transition into the phase with the broken SU(N) symmetry. This ensures the presence of $2(N-1)$ Goldstone states n^l, $l=1,...(N-1)$. The photon remains an auxiliary field, no kinetic term is generated for it. As a result, there is no Coulomb/confining linear rising potential between the n-states. The phase with the broken SU(N) is a deconfinemet phase. Since $|n^l|$ is positively defined Eq. (3.4.3) shows that this phase appears at $L<1/\Lambda_{\rm CP}$.

The results of numerical calculations are in agreement with our conclusions. The relation between orientational energies in both phases is shown in Fig. (3.5). One can see that the Lüscher term energy is lower and is thus physical.

The phase with the broken symmetry in two dimensions can occur only in the limit $N\to\infty$. As was already explained, if N is large but finite this would contradict the Coleman theorem [39]. Therefore, we expect that at large but finite N the phase transition becomes a rapid crossover. In particular, we expect that the n^l fields are not strictly massless. They have small masses suppressed by $1/N$.

To conclude this section let us note that the $CP(N-1)$ model compactified on a cylinder with the so-called twisted boundary conditions was studied in [45]. No phase transition was found; moreover, it was shown that the theory has a mass gap which shows no L-dependence and is determined entirely by $\Lambda_{\rm CP}$. We believe that our results are not in contradiction with those obtained in [45], because at finite L the boundary

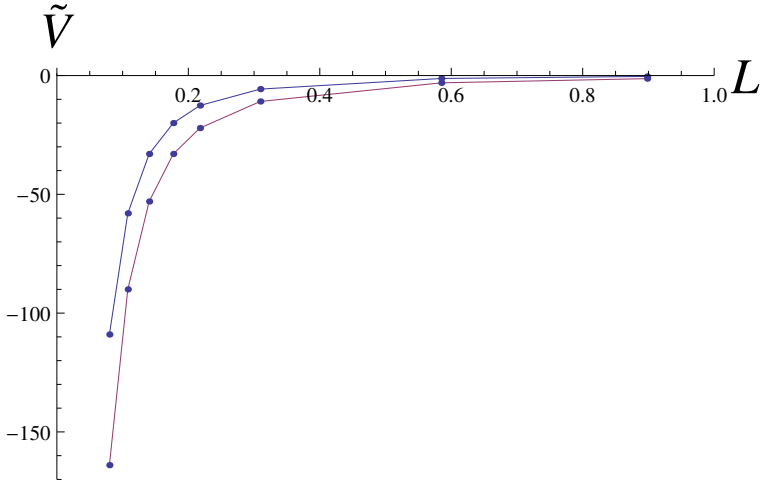

Figure 3.5: Comparison of orientational energies in both phases. The Lüscher term always lies lower. We set $\Lambda_{\rm CP} = 1$.

conditions matter: they can be crucial. In particular, the twisted boundary conditions can be viewed as a gauging of the global SU(N) group with a constant gauge potential. Then the global SU(N) is explicitly broken. This model should be considered as distinct as compared to the CP($N-1$) model with the periodic boundary conditions studied here.

3.5 Supersymmetric CP($N-1$) model with no compactification

Non-Abelian strings were first found in $\mathcal{N} = 2$ supersymmetric QCD with the U(N) gauge group and $N_f = N$ quark hypermultiplets [4, 5, 6, 7], see [8, 9, 10, 11] for reviews. In much the same way as for non-supersymmetric case the internal dynamics of orientational zero modes of non-Abelian string is described by two-dimensional CP($N-1$) model living on the string world-sheet. The string solution is 1/2-BPS saturated; therefore the two-dimensional model under consideration is $\mathcal{N} = (2,2)$ supersymmetric. In this section we briefly review the large-N solution of $\mathcal{N} = (2,2)$ CP($N-1$) model in infinite space [26]. In the next section we will present the large-N solution of the model on a strip of a finite length L (cylindrical compactification).

The bosoinc part of the action of the CP($N-1$) model is given by

$$\begin{aligned} S_{bos} &= \int d^2x \Big[|\nabla_i n^l|^2 + \frac{1}{4e^2} F_{ij}^2 + \frac{1}{e^2} |\partial_i \sigma|^2 + \frac{1}{2e^2} D^2 \\ &+ 2|\sigma|^2 |n^l|^2 + iD(|n^l|^2 - r_0) \Big] , \end{aligned} \tag{3.5.1}$$

where the covariant derivative is defined as $\nabla_i = \partial_i - iA_i$ and σ is a complex scalar field, the scalar superpartner of A_i. Moreover, r_0 is the bare coupling constant. In the limit $e^2 \to \infty$ the gauge field A_i and σ become auxiliary fields. D stands for the D component of the gauge multiplet. The factor i is due to the passage to the Euclidean notation.

The fermionic part of the action takes the form

$$\begin{aligned} S_{ferm} &= \int d^2x \Big[\bar{\xi}_{lR} i(\nabla_0 - i\nabla_3) \xi_R^l + \bar{\xi}_{lL} i(\nabla_0 + i\nabla_3) \xi_L^l \\ &+ \frac{1}{e^2} \bar{\lambda}_R i(\nabla_0 - i\nabla_3) \lambda_R + \frac{1}{e^2} \bar{\lambda}_L i(\nabla_0 + i\nabla_3) \lambda_L \\ &+ \Big(i\sqrt{2} \sigma \bar{\xi}_{lR} \xi_L^l + i\sqrt{2} \bar{n}_l (\lambda_R \xi_L^l - \lambda_L \xi_R^l) + \text{H.c.} \Big) \Big] , \end{aligned} \tag{3.5.2}$$

where the fields $\xi_{L,R}^l$ are the fermion superpartners of n^l and $\lambda_{L,R}$ belong to the gauge multiplet. In the limit $e^2 \to \infty$ they enforce the following constraints:

$$\bar{n}^l \xi_L^l = 0 , \quad \bar{n}^l \xi_R^l = 0 . \tag{3.5.3}$$

The field σ is auxiliary and can be eliminated, namely,

$$\sigma = -\frac{i}{\sqrt{2} r_0} \bar{\xi}_{lL} \xi_R^l . \tag{3.5.4}$$

3.5.1 Large-N solution

The $\mathcal{N} = (2,2)$ supersymmetric CP($N-1$) model was solved in the large-N limit by Witten [26], see also [46]. In this section we briefly review this solution.

Since both fields n^l and ξ^l appear quadratically we can integrate them out. This produces two determinants,

$$\det{}^{-N} \left(-\partial_i^2 + iD + 2|\sigma|^2 \right) \det{}^{N} \left(-\partial_i^2 + 2|\sigma|^2 \right) \tag{3.5.5}$$

The first determinant comes from the boson n^l fields, while the second comes from the fermion ξ^l fields. Note that if $D = 0$ the two contributions obviously cancel each other, and supersymmetry is unbroken. As before, the non-zero values of $iD + 2|\sigma|^2$ and $2|\sigma|^2$ can be interpreted as non-zero values of the mass of n^l and ξ^l fields, and we put $A_k = 0$.

The final expression for the effective potential is given by (see, for example, [46])

$$V_{\text{eff}} = \int d^2x \frac{N}{4\pi} \left[-(iD + 2|\sigma|^2) \ln \frac{iD + 2|\sigma|^2}{\Lambda_{CP}^2} + iD + 2|\sigma|^2 \ln \frac{2|\sigma|^2}{\Lambda_{CP}^2} \right], \tag{3.5.6}$$

where the logarithmic ultraviolet divergence of the coupling constant is traded for the scale Λ_{CP}.

To find a saddle point we minimize the potential with respect to D and σ, which yields the following set of equations:

$$\ln \frac{iD + 2|\sigma|^2}{\Lambda_{CP}^2} = 0\,,$$

$$\ln \frac{iD + 2|\sigma|^2}{2|\sigma|^2} = 0\,, \tag{3.5.7}$$

The solution to these equations is

$$D = 0, \tag{3.5.8}$$

which shows that supersymmetry is not broken. The VEV of σ is

$$\sqrt{2}\sigma = \Lambda_{CP}\, e^{\frac{2\pi k}{N} i}, \qquad k = 0, ..., (N-1). \tag{3.5.9}$$

We see that σ develops a VEV giving masses to the n^l fields and their fermion superpartners ξ^l. The phase factor in the right-hand side of (3.5.9) does not follow from (3.5.7). It comes from the broken chiral U(1) symmetry. The axial anomaly breaks it down to Z_{2N}. The field σ has the chiral charge 2. This explains the phase factor in (3.5.9). Once $|\sigma|$ has a nonzero VEV the anomalous symmetry breaking ensures that the theory has N vacuum states. Clearly this fine structure cannot be seen in the large N approximation since the phase factor is a $1/N$ effect.

In full accord with the Witten index, the solution above has N vacua, each with the vanishing energy.

Consider now the vector multiplet. In much the same way as in the non-supersymmetric case, photon becomes a propagating field. To find the renormalized gauge coupling one needs to evaluate two Feynman diagrams shown in the Fig.3.6.

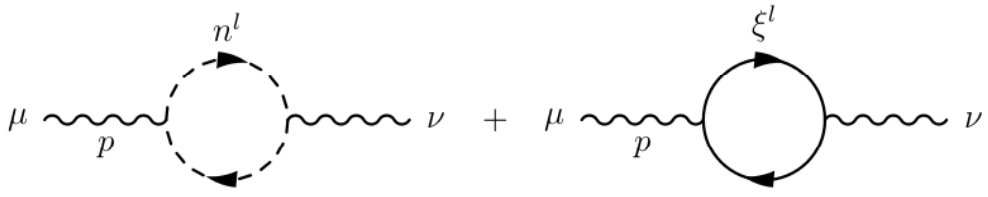

Figure 3.6: Feynman diagrams contributing to the kinetic term of the photon

Details of the appropriate calculation are given in Appendix C. The result is

$$\frac{1}{e^2} = \frac{N}{4\pi}\frac{1}{\Lambda^2_{\rm CP}}\,. \tag{3.5.10}$$

Through the coupling to the $\mathrm{Im}\,\sigma$ (due to the chiral anomaly) now the photon acquires a mass. Moreover, the fermion fields $\lambda_{L,R}$ also become propagating, with the same mass as that of the photon, as required by supersymmetry. The masses of the fields of the vector multiplet are as follows [26, 46]:

$$m_{ph} = m_{\lambda_{L,R}} = m_{\mathrm{Re}\,\sigma} = m_{\mathrm{Im}\,\sigma} = 2\Lambda_{CP}\,. \tag{3.5.11}$$

Since the photon became massive there is no linear rising Coulomb potential between the charged states. There is no confinement in supersymmetric CP$(N-1)$ model even in the infinite volume limit. It has N degenerate vacua which are interpreted as N degenerate elementary non-Abelian strings in the four-dimensional bulk theory. In contrast to the non-supersymmetric case, the confined monopoles of the bulk theory, which are seen as kinks interpolating between the CP$(N-1)$ vacua, are free to move along the string, see [10] for further details.

3.6 Supersymmetric CP$(N-1)$ on a cylinder

Now we compactify one space dimension and impose periodic boundary conditions, both for bosons and fermions, in order to preserve $\mathcal{N}=(2,2)$ supersymmetry. We stress that this compactification can*not* be considered as thermal. Non-zero temperature requires anti-periodic boundary conditions for fermions, which would break supersymmetry explicitly.

The large-N method in the case of $\mathcal{N}=(2,2)$ CP$(N-1)$ model works similar to that in the non-supersymmetric case. We compactify now the spatial coordinate x_1 and start from a slightly modified expression for the determinants in Eq. (3.5.5). Choosing the $A_0=0$ gauge and assuming that A_1 is non-zero we write

$$\det{}^{-N}\left(-\partial_0^2-(\partial_1-iA_1)^2+m_b^2\right)\det{}^{N}\left(-\partial_0^2-(\partial_1-iA_1)^2+m_f^2\right)\,, \tag{3.6.1}$$

where we introduced the following notation:

$$m_b^2=iD+2|\sigma|^2,\qquad m_f^2=2|\sigma|^2. \tag{3.6.2}$$

The evaluation of each of the determinants is no different from that in the non-supersymmetric case. Again we use the zeta-function method. Using expressions in Appendix C we can derive the effective potential,

$$\begin{aligned} E &= \frac{LN}{4\pi}\Big[-(iD+2|\sigma|^2)\ln\frac{iD+2|\sigma|^2}{\Lambda_{\rm CP}^2}+iD+2|\sigma|^2\ln\frac{2|\sigma|^2}{\Lambda_{\rm CP}^2} \\ &- 8m_b^2\sum_{k=1}^{\infty}\frac{K_1(Lm_bk)}{Lm_bk}\cos\left(LA_1k\right) \\ &+ 8m_f^2\sum_{k=1}^{\infty}\frac{K_1(Lm_fk)}{Lm_fk}\cos\left(LA_1k\right)\Big]\,, \end{aligned} \tag{3.6.3}$$

Here the first line is just the effective potential at $L=\infty$, while the second and third lines are the finite-L corrections due to bosons and fermions, respectively.

To find a stationary point we vary the above expression with respect to A_1, D and σ. The resulting equations are as follows:

$$\begin{aligned} &m_b\sum_{k=1}^{\infty}K_1(Lm_bk)\sin\left(LA_1k\right)-m_f\sum_{k=1}^{\infty}K_1(Lm_fk)\sin\left(LA_1k\right)=0\,, \\ &2\sigma\left[-\ln\frac{m_b^2}{m_f^2}+4\sum_{k=1}^{\infty}K_0(Lm_bk)\cos\left(LA_1k\right)-4\sum_{k=1}^{\infty}K_0(Lm_fk)\cos\left(LA_1k\right)\right]=0\,, \\ &-\ln\frac{m_b^2}{\Lambda_{CP}^2}+4\sum_{k=1}^{\infty}K_0(Lm_bk)\cos\left(LA_1k\right)=0\,. \end{aligned} \tag{3.6.4}$$

Calculation of the gauge coupling constant at finite L is also modified (see Appendix C). As a result, we arrive at

$$\frac{1}{Ne^2} = \frac{1}{4\pi m_b^2} + \frac{L}{2\pi m_b}\sum_{k=1}^{\infty} K_1(Lm_b k)k\,, \tag{3.6.5}$$

which reduces to $1/4\pi\Lambda_{\rm CP}^2$ in the limit $L\to\infty$.

Consider now the large L limit, $L \gg 1/\Lambda_{\rm CP}$. Assuming that $m_b \sim m_f \sim \Lambda_{\rm CP}$ (we confirm this below) we expand the string energy (3.6.3) keeping the first exponentially small term

$$\begin{aligned} E &= \frac{LN}{4\pi}\left\{-m_b^2\ln\frac{m_f^2}{\Lambda_{\rm CP}^2} + iD + m_f^2\ln\frac{m_f^2}{\Lambda_{\rm CP}^2}\right\} \\ &- N\sqrt{\frac{2}{\pi}}\left[\sqrt{\frac{m_b}{L}}\,e^{-m_b L} - \sqrt{\frac{m_f}{L}}\,e^{-m_f L}\right]\cos A_1 L + \cdots\,. \end{aligned} \tag{3.6.6}$$

Taking derivatives with respect to D, $\sqrt{2}\bar\sigma$ and A_1 we obtain

$$\begin{aligned} &-\frac{N}{4\pi}\log\frac{m_b^2}{\Lambda_{CP}^2}^{\,2} + N\,\frac{1}{\sqrt{2\pi}}\,\frac{\exp\left(-m_b L\right)}{\sqrt{m_b L}}\,\cos A_1 L + \cdots = 0, \\ &\sqrt{2}\sigma\left\{\frac{N}{4\pi}\log\frac{m_f^2}{m_b^2} + N\,\frac{1}{\sqrt{2\pi}}\left[\frac{\exp\left(-m_b L\right)}{\sqrt{m_b L}} - \frac{\exp\left(-m_f L\right)}{\sqrt{m_f L}}\right]\cos A_1 L + \cdots\right\} = 0, \\ &\left\{\frac{\exp\left(-m_b L\right)}{\sqrt{m_b L}} - \frac{\exp\left(-m_f L\right)}{\sqrt{m_f L}}\right\}\sin A_1 L + \cdots = 0\,, \end{aligned} \tag{3.6.7}$$

where the ellipses denote next-to-leading corrections in $1/Lm_b$ and $1/Lm_f$.

The solution of these equations is as follows. The second and third equations are satisfied at

$$D = 0, \tag{3.6.8}$$

which shows that supersymmetry is not broken. A_1 remains undetermined.

With $D=0$ the first equation determines the σ expectation value, namely,

$$\frac{N}{4\pi}\log\frac{2|\sigma|^2}{\Lambda_{\rm CP}^2} = N\,\frac{1}{\sqrt{2\pi}}\,\frac{\exp\left(-\sqrt{2}|\sigma|L\right)}{\sqrt{\sqrt{2}|\sigma|L}}\,\cos A_1 L + \cdots\,. \tag{3.6.9}$$

This equation seems to present a puzzle. It shows that the VEV of σ depends on the parameter A_1, which is arbitrary. If this were the case the theory would have a branch of vacua parametrized by the Polyakov line

$$e^{\int dx_1 A_1} = e^{iA_1 L}, \tag{3.6.10}$$

which measures the holonomy around the compact dimension. More exactly, the theory would have N branches of vacua, because Z_{2N} symmetry ensures that the overall phase of σ takes N values $2\pi k/N$, $k = 0, ..., (N-1)$. This would contradict the Witten index argument which ensures that the number of vacua is equal to N for $\mathcal{N} = (2,2)$ supersymmetric CP$(N-1)$ model.

The resolution of this puzzle is that we should quantize the phase variable $A_1 L$ (note that $\int dx_1 A_1$ depends only on time) as a function of the non-compact time. In the emerging quantum mechanics the phase $A_1 L$ is not fixed; instead, it is smeared all over the circle (in the ground state). As a result, the $\cos(A_1 L)$ in (3.6.9) is averaged to zero and the σ VEVs are given by

$$\sqrt{2}\sigma = \Lambda_{\rm CP}\, e^{\frac{2\pi k}{N} i}, \qquad k = 0, ..., (N-1). \tag{3.6.11}$$

This is exactly the same result as for $L = \infty$. All cosine functions of $A_1 L$ in the last equation in (3.6.4) are averaged to zero, therefore the result in (3.6.11) is exact and does not depend on L.

This result also can be understood by studying the exact twisted superpotential of $\mathcal{N} = (2,2)$ CP$(N-1)$ model. In the infinite volume it is given by [47, 48, 49]

$$W(\sigma) = \frac{N}{4\pi}\left\{\sqrt{2}\sigma\, \log\frac{\sqrt{2}\sigma}{\Lambda_{\rm CP}} - \sqrt{2}\sigma\right\}. \tag{3.6.12}$$

This superpotential has correct transformation properties with respect to the chiral U(1) symmetry. Namely, integrated over half of the superspace it is invariant under chiral symmetry up to a term which precisely reproduces the chiral anomaly. Now at finite length this superpotential in principle could have corrections proportional to powers of

$$\exp\left(-\sqrt{2}\sigma L\right). \tag{3.6.13}$$

However these corrections would spoil the transformation properties of the superpotential with respect to the chiral symmetry. Therefore they are forbidden. As a result at

finite L the exact superpotential of the theory is still given by (3.6.12). Critical points of this superpotential are given by (3.6.11) and do not depend on L. This matches our result obtained from large-N approximation.

In particular, at small L the theory is at weak coupling and can be studied in the quasiclassical approximation. As we already mentioned CP($N-1$) model compactified on a cylinder with twisted boundary conditions was studied in [45]. It is shown in [45] that the mass gap at weak coupling is produced by fractional instantons and does not depend on L both in supersymmetric and non-supersymmetric cases. For our case (periodic boundary conditions) the mass gap shows L-dependence in non-supersymmetric case, while in the supersymmetric case it is L-independent. The quasiclassical origin of this behavior needs to be understood in the weak coupling domain of small L. This is left to a future work.

To conclude, in $\mathcal{N}=(2,2)$ supersymmetric CP($N-1$) model we have a *single* phase with the unbroken supersymmetry and N vacua. Each vacuum has vanishing energy and parametrized by the VEV of σ in Eq. (3.6.11). Unlike non-supersymmetric problem, this VEV is independent of L.

3.7 The photon mass

In this section we outline the photon mass calculation.

The effective action for the gauge field can be written as [46]

$$S_{\rm gauge} = \int d^2x \left\{ \frac{1}{4e^2}\, F_{kl}^2 - \frac{N}{4\pi}\, \log\frac{\sigma}{\bar\sigma}\, F^* \right\}, \tag{3.7.1}$$

where the photon mixing with σ is due to the chiral anomaly and

$$F^* = \frac{1}{2}\epsilon_{ij}F^{ij} \tag{3.7.2}$$

is the dual gauge field strength. In the case of infinitely long string the the gauge coupling and the photon mass were found [46],

$$\frac{1}{e^2} = \frac{N}{4\pi}\frac{1}{\Lambda_{CP}^2}\,, \tag{3.7.3}$$

and

$$m_{ph} = 2\Lambda_{CP}\,, \tag{3.7.4}$$

respectively. In Sec. 3.6 we derived the expression for the gauge coupling in the case of finite length, see (3.6.5). The corresponding expression for the photon mass in the limit of $\Lambda_{CP}L \gg 1$ is

$$m_{\rm ph}^2 \approx (2\Lambda_{\rm CP})^2 \left(1 - \sqrt{2\pi\Lambda_{\rm CP}L}\, e^{-\Lambda_{\rm CP}L}\right) \tag{3.7.5}$$

where we used the asymptotic expansion of the modified Bessel functions (see Eq. (9.7.2) in [43]),

$$K_1(x) \sim \sqrt{\frac{\pi}{2x}} e^{-x}\,. \tag{3.7.6}$$

Since $K_0'(x) = -K_1(x)$ we can also determine the photon mass in the opposite limit of $\Lambda_{\rm CP}L \ll 1$,

$$\begin{aligned} \sum_{k=1}^{\infty} K_1(kx)k &= -\left(\sum_{k=1}^{\infty} K_0(kx)\right)' \approx \frac{\pi}{2x^2} - \frac{1}{2x}\,, \\ m_{\rm ph}^2 &\approx \frac{\Lambda_{\rm CP}L}{\pi}\,(2\Lambda_{\rm CP})^2 \ll (2\Lambda_{\rm CP})^2\,. \end{aligned} \tag{3.7.7}$$

Chapter 4

Heterotic Non-Abelian String

4.1 Heterotic $\mathcal{N} = (0,2)$ CP$(N-1)$ model at $L = \infty$

The heterotic $\mathcal{N} = (0,2)$ CP$(N-1)$ model at $L = \infty$ was solved in [46] in the large-N limit. In this section we will briefly review this solution. The bosonic part of the action in the gauged formulation is

$$S_b = \int d^2x \Big[|\nabla_k n^l|^2 + 2|\sigma|^2 |n^l|^2 + iD(|n^l|^2 - r_0) + 4|\omega|^2 |\sigma|^2 \Big] , \tag{4.1.1}$$

where n^l $(l = 1, ...N)$ is a complex N-vector parametrizing the orientational modes. Moreover,

$$\nabla_k = \partial_k - iA_k \, .$$

Here A_k is the gauge potential, σ is a complex scalar field. The fields A_k, σ and D belong to the gauge (vector) multiplet. These fields come without kinetic terms and are auxiliary. Moreover, r_0 is a coupling constant, while ω is the $\mathcal{N} = (2,2)$ deformation parameter. Eliminating D leads to the constraint

$$|n^l|^2 = r_0 \, . \tag{4.1.2}$$

The fermionic part of the action is

$$\begin{aligned} S_f &= \int d^2x \Big[\bar{\xi}_{lR} i(\nabla_0 - i\nabla_3)\xi^l_R + \bar{\xi}_{lL} i(\nabla_0 + i\nabla_3)\xi^l_L \\ &+ i\sqrt{2}\sigma\bar{\xi}_{lR}\xi^l_L + i\sqrt{2}\bar{n}^l(\lambda_R\xi^l_L - \lambda_L\xi^l_R) \\ &+ i\sqrt{2}\sigma^\star\bar{\xi}_{lL}\xi^l_R + i\sqrt{2}(\bar{\lambda}_L\bar{\xi}^l_R - \bar{\lambda}_R\bar{\xi}^l_L)n^l \\ &+ \frac{1}{2}\bar{\zeta}_R i\partial_L\zeta_R + (i\sqrt{2}\omega\bar{\lambda}_L\zeta_R + \text{H.c.})\Big] , \end{aligned} \tag{4.1.3}$$

where $\xi^l_{R,L}$ are fermionic superpartners of n^l (superorientational modes of the string), $\lambda_{R,L}$ are auxiliary fermions from the vector superfield, while ζ_R is the right-handed supertranslational mode. In the $\mathcal{N} = (2,2)$ model it was decoupled. We do not include the bosonic translational modes describing shifts of the string center. Nor do we include the left-handed supertranslational mode ζ_L, because both decouple not only in the $\mathcal{N} = (2,2)$ but in the $\mathcal{N} = (0,2)$ model as well [28, 29].

The terms containing ζ_R or ω break $\mathcal{N} = (2,2)$ down to $\mathcal{N} = (0,2)$. The deformation parameter ω is complex and scales with N as [46]

$$\omega \sim \sqrt{N} . \tag{4.1.4}$$

It is determined by the mass parameter of the adjoint matter in the bulk theory [29].

Integrating over $\lambda_{L,R}$ leads to the constraints

$$\begin{aligned} \bar{n}^l\xi^l_L &= 0 , \\ \bar{\xi}_R n^l &= \omega\zeta_R . \end{aligned} \tag{4.1.5}$$

Integrating over σ implies

$$\sigma = -\frac{i}{\sqrt{2}(r_0 + 2|\omega|^2)}\bar{\xi}_{lL}\xi^l_R . \tag{4.1.6}$$

Note that this model has an axial $U(1)$ symmetry broken by the chiral anomaly down to Z_{2N} much in the same way as in the $\mathcal{N} = (2,2)$ model [26]. We find that σ develops a vacuum expectation value (VEV) which results in a spontaneous breaking of the discrete Z_{2N} down to Z_2. Moreover as can be seen from (4.1.6), a non-zero VEV of the σ field corresponds to a non-zero fermion bilinear condensate $\langle\bar{\xi}_{lL}\xi^l_R\rangle$.

Since both fields n^l and ξ^l appear in the action quadratically we can integrate them out. This produces the product of two determinants,

$$\det{}^{-N}\left(-\partial_i^2 + iD + 2|\sigma|^2\right)\det{}^{N}\left(-\partial_i^2 + 2|\sigma|^2\right). \tag{4.1.7}$$

The first determinant comes from the boson n^l fields, while the second comes from the fermion ξ^l fields. Note that if $D = 0$ the two contributions obviously cancel each other, and supersymmetry is unbroken. Also, the non-zero values of $iD + 2|\sigma|^2$ and $2|\sigma|^2$ can be interpreted as non-zero values of the masses of the n^l and ξ^l fields, respectively. We put $A_k = 0$.

The final expression for the effective potential is (see [46])

$$\begin{aligned} V_{\text{eff}} &= \int d^2x \frac{N}{4\pi}\Bigg[-(iD + 2|\sigma|^2)\ln\frac{iD + 2|\sigma|^2}{\Lambda^2} + iD \\ &+ 2|\sigma|^2 \ln\frac{2|\sigma|^2}{\Lambda^2} + 2|\sigma|^2 u\Bigg], \end{aligned} \tag{4.1.8}$$

where the logarithmic ultraviolet divergence of the coupling constant is traded for the finite scale Λ of the asymptotically free CP$(N-1)$ model. We also introduced a dimensionless deformation parameter

$$u = \frac{8\pi}{N}|\omega|^2, \tag{4.1.9}$$

which does not scale with N.

To find the saddle point we minimize the potential with respect to D and σ, which yields the following set of equations:

$$\begin{aligned} \ln\frac{iD + 2|\sigma|^2}{\Lambda_{CP}^2} &= 0, \\ \ln\frac{iD + 2|\sigma|^2}{2|\sigma|^2} &= u. \end{aligned} \tag{4.1.10}$$

The solution to these equations is

$$iD = \Lambda^2(1 - e^{-u}), \quad \text{and} \quad 2|\sigma|^2 = \Lambda^2 e^{-u}. \tag{4.1.11}$$

The value of D in this solution does not vanish, implying that supersymmetry is spontaneously broken. We see that σ develops a VEV giving masses to the n^l fields and

their fermion superpartners ξ^l. More exactly, the solution for σ can also be written as

$$\sqrt{2}\sigma = \Lambda \exp\left(-\frac{u}{2} + \frac{2\pi i k}{N}\right), \quad k = 0, ..., N-1\,, \tag{4.1.12}$$

where the phase factor is not seen in Eq. (4.1.10). It comes as a result of a chiral anomaly which breaks the chiral U(1) symmetry, U(1) $\to Z_{2N}$. The field σ has the chiral charge 2. Thus a non-zero VEV of $|\sigma|$ ensures that Z_{2N} symmetry is broken down to Z_2 and there are N vacua presented in (4.1.12).

Substituting the solution (4.1.10) into (4.1.8) we obtain an expression for the vacuum energy density

$$V_{\rm vac} = \frac{N}{4\pi}\Lambda^2(1 - e^{-u})\,, \tag{4.1.13}$$

which, as expected, vanishes in the limit $u \to 0$.

4.2 $\mathcal{N} = (0, 2)$ model on a cylinder

The $\mathcal{N} = (2, 2)$ model on a cylinder was solved in the large-N limit in the previous Chapter. In this section we apply the same approach to $\mathcal{N} = (0, 2)$ model assuming periodic boundary conditions both for bosons and fermions. Since the action (4.1.1) and (4.1.3) is quadratic in n^l and ξ^l we can integrate over these fields. We assume that the compact dimension in the bulk theory is x_1 and the string is wrapped around this dimension. We will assume a nontrivial holonomy (3.6.10) of A_k around this compact dimension. In the $A_0 = 0$ gauge we will look for a solution with $A_1 = \text{const}$.

First consider the case when neither of the fields n^l or ξ^l develop VEVs. The expression for the effective potential is easily found,

$$\begin{aligned} V &= \frac{N}{4\pi}\Big(iD - iD\ln\frac{m_b^2}{\Lambda^2} - m_f^2\ln\frac{m_b^2}{m_f^2} + m_f^2 u \\ &+ 8m_f^2\sum_{k=1}^{\infty}\frac{K_1(Lm_f k)}{Lm_f k}\cos LkA_1 \\ &- 8m_b^2\sum_{k=1}^{\infty}\frac{K_1(Lm_b k)}{Lm_b k}\cos LkA_1\Big)\,, \end{aligned} \tag{4.2.1}$$

where we use an effective mass notation for the bosonic n^l and fermionic ξ^l fields,

$$m_b^2 = iD + 2|\sigma|^2, \qquad m_f^2 = 2|\sigma|^2,\,. \tag{4.2.2}$$

Here $K_1(z)$ is the modified Bessel function of the second kind and the deformation parameter u is related to the parameter ω as in (4.1.9). The first line in (4.2.1) is the same as the one found in the case of the $L = \infty$ string (4.1.8), while the second and third lines represent contributions arising due to the finite length of the string. The potential (4.2.1) is periodic in the phase LA_1, with the period 2π, so we can assume that $0 \leq LA_1 < 2\pi$.

4.2.1 Saddle point approximation

To find VEVs of A_1, of σ and iD we take derivatives of (4.2.1) with respect to these fields. Then we obtain three equations,

$$\begin{aligned} V_{N,A_1} &= m_b \sum_{k=1}^{\infty} K_1(Lm_b k) \sin LkA_1 - m_f \sum_{k=1}^{\infty} K_1(Lm_f k) \sin LkA_1 \,, \\ V_{N,\sigma^\star} &= 2\sigma \left[-\ln \frac{m_b^2}{m_f^2} + 4 \sum_{k=1}^{\infty} K_0(Lm_b k) \cos LkA_1 \right. \\ &- \left. 4 \sum_{k=1}^{\infty} K_0(Lm_f k) \cos LkA_1 + u \right] , \\ V_{N,iD} &= -\ln \frac{m_b^2}{\Lambda^2} + 4 \sum_{k=1}^{\infty} K_0(Lm_b k) \cos LkA_1 \,. \end{aligned} \tag{4.2.3}$$

One can see that the first equation is satisfied when either $A_1 = 0$ or $A_1 = \pi/L$. However, unlike the bosonic theory described in the previous Chapter, $A_1 = 0$ corresponds to the maximum of potential. The energy is lower if $LA_1 = \pi$. This can be easily understood. Consider the second and third lines in (4.2.1),

$$V_A \sim [m_f K_1(Lm_f) - m_b K_1(Lm_b)] \cos(LA_1) \,. \tag{4.2.4}$$

On the one hand we know from the definition that $m_b \geq m_f$. On the other hand $K_1(x)$ decreases exponentially at large values of the argument. Thus, at least for large L the potential $E_A = c \times \cos(LA_1)$, where $c > 0$. Hence we conclude that the minimum of the potential is at $LA_1 = \pi$. This conclusion is also supported by a numerical calculation, see Figs. 2,3. Below we assume that

$$LA_1 = \pi \,. \tag{4.2.5}$$

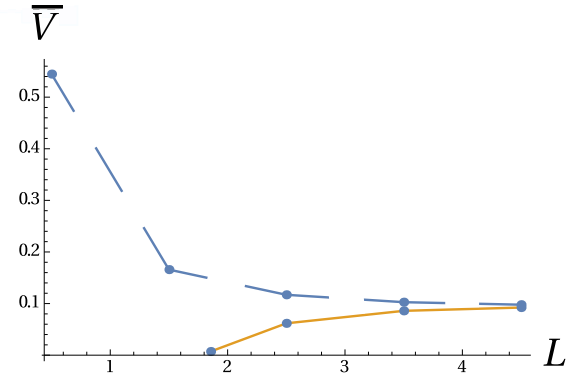

Figure 4.1: $\bar{V} \equiv 4\pi V$ vs string length L at the value of deformation parameter $u = 0.1$. Solid line corresponds to $A_1 = \pi/L$, while dashed line correcponds to $A_1 = 0$.

As can be seen from the graphs in Figs. 2, 3 no solution with lower energy exists for sufficiently small L and/or high enough value of the deformation parameter. To explore this issue we need to find approximate analytical solutions.

4.3 Z_{2N} broken phase

Consider first the large-L domain or, more precisely, $L \gg 1/\Lambda$. In addition we assume that u is not very large. Then we use the second and third equations in (4.2.3) to find the expressions for masses. Next, we use (4.2.1) to find the vacuum energy.

We will show below that in the limit of large $L\Lambda \gg 1$ and intermediate u we have $Lm_{b,f} \gg 1$. If so, to find the boson and fermion masses we can apply the asymptotic behavior of the modified Bessel functions,

$$K_0(z) \approx K_1(z) \approx \sqrt{\frac{\pi}{2z}} e^{-z} \,. \tag{4.3.1}$$

Assuming that $LA_1 = \pi$ we arrive at the following expressions for masses:

$$\begin{aligned} m_b^2 &\approx \Lambda^2 \left(1 - \sqrt{\frac{8\pi}{\Lambda L}} e^{-\Lambda L}\right) , \\ m_f^2 &\approx \Lambda^2 e^{-u} \left\{1 - \sqrt{\frac{8\pi}{\Lambda L}} e^{\frac{u}{4}} e^{-\Lambda L e^{-u/2}}\right\} . \end{aligned} \tag{4.3.2}$$

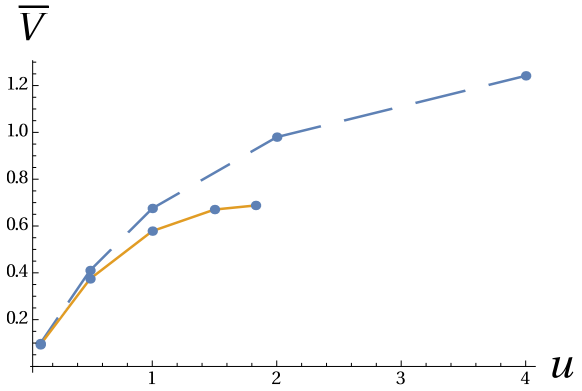

Figure 4.2: $\bar{V} \equiv 4\pi V$ vs deformation parameter u at the sting length $L = 4.5$.

If L is large, $L\Lambda \gg 1$, and the value of u is neither too large nor too small, exponential corrections are small and $m_{b,f}$ are of order of Λ. This justifies our approximation. As was already mentioned, m_b and m_f have a meaning of masses for bosons n^l and fermions ξ^l. Thus we have a non-vanishing mass gap in this phase.

From (4.3.2) we find VEVs of D and σ,

$$\begin{aligned} iD &\approx \Lambda^2 \left\{ 1 - e^{-u} - \sqrt{\frac{8\pi}{\Lambda L}} \left(e^{-\Lambda L} - e^{-3u/4} e^{-\Lambda L e^{-u/2}} \right) \right\} , \\ \sqrt{2}\sigma &\approx \Lambda\, e^{-\frac{u}{2}} \left\{ 1 - \sqrt{\frac{2\pi}{\Lambda L}} e^{\frac{u}{4}} e^{-\Lambda L e^{-u/2}} \right\} e^{\frac{2\pi i k}{N}} , \end{aligned} \tag{4.3.3}$$

where $k = 0, ..., (N-1)$.

The presence of non-zero D signals that $\mathcal{N} = (0,2)$ supersymmetry is spontaneously broken. The vacuum energy is

$$E \approx \frac{NL\Lambda^2}{4\pi} \left\{ 1 - e^{-u} + \frac{2}{\Lambda L} \sqrt{\frac{8\pi}{\Lambda L}} \left(e^{-\Lambda L} - e^{-u/4} e^{-\Lambda L e^{-u/2}} \right) \right\} . \tag{4.3.4}$$

The phase of σ in (4.3.3) is determined by the same phase factor as in (4.1.12). We see that we have N degenerative vacua, in much the same way as in the infinite volume case. The degeneracy is not due to supersymmetry but due to the fact that the discrete chiral Z_{2N} symmetry is broken down to Z_2.

Our approximation assumes that both boson and fermion masses are large as compared to $1/L$. However, from (4.3.2) we see that m_f exponentially decreases at large u. Our approximation breaks down when we increase u above the curve

$$L\Lambda \sim e^{\frac{u}{2}}. \tag{4.3.5}$$

We will see in Sec. 4.4 that in fact on this curve σ becomes zero and the theory goes into Z_{2N}-symmetric phase.

4.3.1 Quantum mechanics: the $u \to 0$ limit

It was shown in Chapter (3) that the VEV of the σ field in the CP$(N-1)$ model with $\mathcal{N}=(2,2)$ supersymmetry does not depend on the string length. Since in L is not a holomorphic parameter, $\mathcal{N}=(2,2)$ supersymmetry forbids the effective twisted superpotential (which determines the σ VEV) to depend on L.

The fact that L is not a holomorphic parameter in $\mathcal{N}=(2,2)$ CP$(N-1)$ model is not a universal statement. Examples are known when L in combination with another variable form a holomorphic quantity. For instance, in the case of $\mathcal{N}=1$ supergravity on $R^3 \times S^1$ considered in [50] the radius of S^1 is combined with the dual photon field into one holomorphic parameter which does enter the expression for the superpotential.

Our problem, however, does not fall in the above class. In $\mathcal{N}=(2,2)$ CP$(N-1)$ there is no additional field to partner with the parameter L to make it holomorphic. The conserved R charge in this model plays a custodial role and precludes L dependence of the superpotential.

More explicitly, one can expect that the effective twisted superpotential can depend on dimensionless parameter σL, however U$(1)_R$ symmetry forbids this dependence. This is because σ has U$(1)_R$ charge equal to 2 while L is neutral [2] . The L independence of the σ condensate ensues.

However, in the heterotic CP$(N-1)$ model supersymmetry is spontaneously broken. Thus one can expect the σ VEV to depend on the string length. This is what we observe in Eq. (4.3.3). However, one can note that the expressions for the boson and fermion masses (4.3.2) in the limit of vanishing u do not reduce to those obtained in

[2] U$(1)_R$ symmetry is broken by chiral anomaly, however one can compensate for this breaking if one assigns R charge equal to 2 to CP$(N-1)$ scale Λ.

the CP($N-1$) model with $\mathcal{N}=(2,2)$ supersymmetry. It depends on the string length even if $u=0$. What is happening?

To resolve this puzzle we note that the $u \to 0$ limit turns out to be in conflict with the quasiclassical approximation in the one-loop effective action which we use in the large-N analysis. We will see below that the relevant parameter is uN^2. Thus, the change of regime we expect to detect occurs at $u \sim 1/N^2$ and is not seen in the standard treatment.

In other words, to detect this change of regimes we must consider a quantum-mechanical problem for the Polyakov line (3.6.10) and average operators $\cos(LkA_1)$ that appear in the equations defining masses (4.2.3) over the ground state wave function. The equations for the masses in the small-u limit become

$$\begin{aligned} \ln \frac{m_b^2}{\Lambda^2} &= 4\sum_{k=1}^{\infty} K_0(Lm_b k)\chi_k \,, \\ \ln \frac{m_f^2}{\Lambda^2} &= 4\sum_{k=1}^{\infty} K_0(Lm_f k)\chi_k - u \,. \end{aligned} \tag{4.3.6}$$

where the χ_k is the average value of the operator $\cos(LkA_1)$ defined as

$$\chi_k = \int_{-\pi}^{\pi} L\, dA_1 |\psi|^2 \cos(LkA_1) \,. \tag{4.3.7}$$

Here ψ is the ground state wave function in quantum mechanics for LA_1.

In this way we obtain the masses

$$\begin{aligned} m_{b\pi}^2 &\approx \Lambda^2 \left(1 + \sqrt{\frac{8\pi}{\Lambda L}} e^{-\Lambda L} \chi_1\right) \,, \\ m_{f\pi}^2 &\approx \Lambda^2 \left(1 + \sqrt{\frac{8\pi}{\Lambda L}} e^{-\Lambda L} \left(1 + \frac{u\Lambda L}{2} - \frac{3u}{4}\right)\chi_1 - u\right) \,, \end{aligned} \tag{4.3.8}$$

where we expand the expressions for masses m_b and m_f at large L and small u. This expressions imply a smooth $\mathcal{N}=(2,2)$ limit if χ_1 vanishes with u.

From equation (4.2.1) one can read off the action for the A_1 quantal variable,

$$\begin{aligned} S = \int dt \Bigg[\frac{L\dot{A}_1^2}{4e^2} &+ \frac{LN}{4\pi}\Bigg(8m_f^2 \sum_{k=1}^{\infty} \frac{K_1(Lm_f k)}{Lm_f k} \cos(LkA_1) \\ &\quad -8m_b^2 \sum_{k=1}^{\infty} \frac{K_1(Lm_b k)}{Lm_b k} \cos(LkA_1)\Bigg)\Bigg] \,. \end{aligned} \tag{4.3.9}$$

In the large-L limit the equation for the wave function is given by

$$\frac{d^2\psi}{d\phi^2} + (\lambda - 2q\cos(2\phi))\psi = 0\,, \tag{4.3.10}$$

where $\phi = LA_1/2$, and the parameter q is defined as follows:

$$q = \frac{uN^2 e^{-\Lambda L}}{(2\pi\Lambda L)^{3/2}}\Lambda L\,, \tag{4.3.11}$$

(please, observe its explicit dependence on uN^2). This is the Mathieu equation. The solution for the wave function can be found numerically. The averaged value of $\cos(LA_1)$ is

$$\begin{aligned}
\chi_1 &= -0.99 \quad \text{at} \quad \Lambda L = 5 \quad \text{and} \quad uN^2 = 10^9 \\
\chi_1 &= -0.85 \quad \text{at} \quad \Lambda L = 5 \quad \text{and} \quad uN^2 = 10^5 \\
\chi_1 &= -10^{-3} \quad \text{at} \quad \Lambda L = 5 \quad \text{and} \quad uN^2 = 10^1\,.
\end{aligned} \tag{4.3.12}$$

Thus we see that for large values of the deformation parameter the averaging plays almost no role, and the saddle point approximation works well. However, as the deformation parameter gets smaller the averaged value of cosine vanishes and the expression for fermion mass reduces to that obtained in the $\mathcal{N} = (2, 2)$ model.

A more transparent albeit qualitative analysis can be carried out if we use the harmonic oscillator approximation in our quantal problem. Then one can find the averaged value of $\cos LA_1$ analytically,

$$\chi_1 \approx -\sqrt{uN^2 e^{-\Lambda L}}\left(\frac{2\pi}{\Lambda L}\right)^{1/4}\,. \tag{4.3.13}$$

This result explicitly demonstrates vanishing of χ_1 as the deformation parameter uN^2 tends to zero. Thus we see that in the $u \to 0$ limit the solution of the $\mathcal{N} = (0, 2)$ model tends to that of the $\mathcal{N} = (2, 2)$ model in the interval $u \in [0, \text{const}/N^2]$.

4.4 The Z_{2N} unbroken phase

Now let us consider the region where u is large, i.e. $u \gg \log \Lambda L$, see Eq. (4.3.5). For the time being we assume that L is still large, $L \gg 1/\Lambda$. We can find approximate analytic

solution for a curve in the $(L,\, u)$ plane at which the Z_{2N} broken phase with N distinct vacua ceases to exist (see the phase diagram in Fig. 1). This phase is terminated when the fermion mass (it is always smaller or equal to the boson mass) reaches zero as we increase u. Assuming that the fermion mass is close to zero so that $Lm_f \ll 1$ we can approximate the sums of the Bessel functions in (4.2.3). Noting that $\cos(\pi k) = (-1)^k$ we use (D.3) with $y = 0$ to obtain the following expression for the fermion mass

$$(Lm_f)^2 S_2 \approx S_1 + \gamma - \ln \frac{4\pi}{\Lambda L} - \frac{u}{2}\,, \tag{4.4.1}$$

where $S_{1,2}$ are defined in (A.3). Thus, the solution with non-zero m_f exists only below the curve

$$\Lambda L \approx 4\pi e^{u/2 - S_1 - \gamma}\,. \tag{4.4.2}$$

This formula gives a more accurate prediction for the curve (4.3.5) which was obtained in the previous section. Moreover, the minimal string length is $\Lambda L \approx 1.76$. Numerical calculation also shows that the fermionic mass goes to zero at finite values of both L and u, as can be seen from Fig. (4.3) and (4.4).

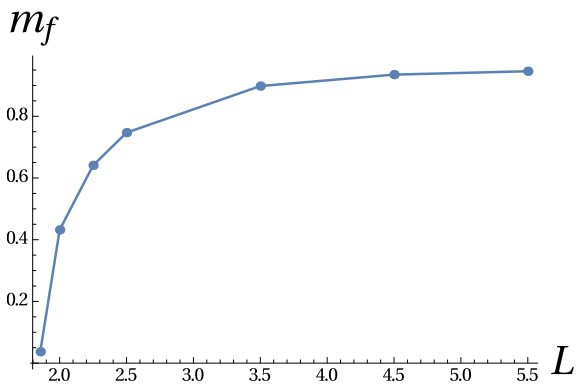

Figure 4.3: Fermion mass m_f vs string length L at the value of the deformation parameter $u = 0.1$.

Moreover it is clear from Figs. 4.3 and 4.5 that as $L \gg 1/\Lambda$ the fermionic mass m_f tends to Λe^{-u} while iD tends to $\Lambda^2(1 - e^{-u})$, in agreement with (4.3.2) and (4.3.3), respectively. One can also note that $iD \to 0$ as $u \to 0$. This is expected since the $u = 0$ limit corresponds to the $\mathcal{N} = (2, 2)$ model.

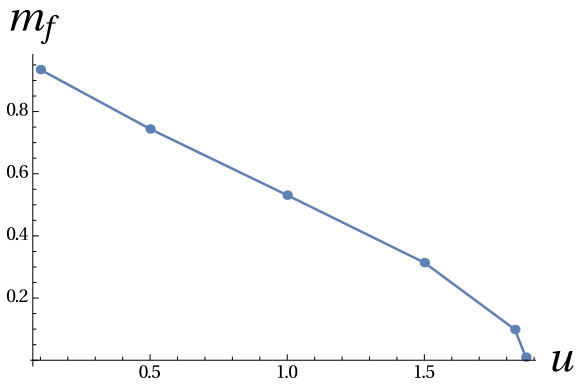

Figure 4.4: Fermion mass m_f vs deformation parameter u at $L = 4.5$.

Above the curve (4.4.2), the only solution of the second equation in (4.2.3) is

$$\sigma = 0\,, \tag{4.4.3}$$

while the boson mass

$$m_b^2 \approx \Lambda^2 \left(1 - \sqrt{\frac{8\pi}{\Lambda L}} e^{-\Lambda L}\right) \tag{4.4.4}$$

is still given by the same expression as in the Z_{2N} broken phase, see (4.3.2).

Note that the Z_{2N} unbroken phase we have observed is quite remarkable. On the phase transition line N vacua fuse to one, a family of split Z_{2N}-symmetric vacua does not emerge. We will discuss this circumstance later.

4.4.1 The Lüscher term.

Using the expression (D.13) from Appendix D we find that the vacuum energy in this phase is independent on u and given by

$$E \approx \frac{LN\Lambda^2}{4\pi} \left(1 + \frac{2}{\Lambda L}\sqrt{\frac{8\pi}{\Lambda L}} e^{-\Lambda L}\right) - \frac{\pi N}{6L}\,. \tag{4.4.5}$$

The second term here is the Lüscher term [24]. It arises due to massless fermions. Note, that it equals to half of what we found for non-supersymmetric theory where it comes from bosons (3.4.4). The reason is that now the gauge holonomy is non-trivial,

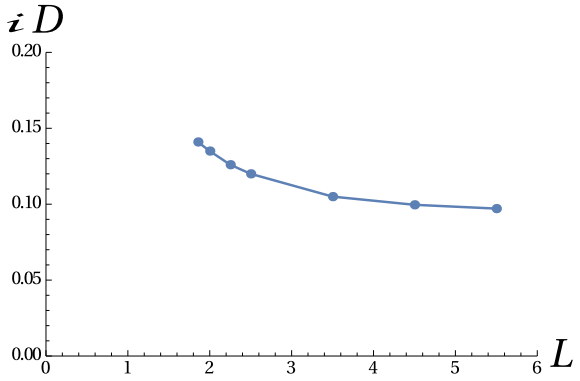

Figure 4.5: iD vs L at the value of the deformation parameter $u = 0.1$.

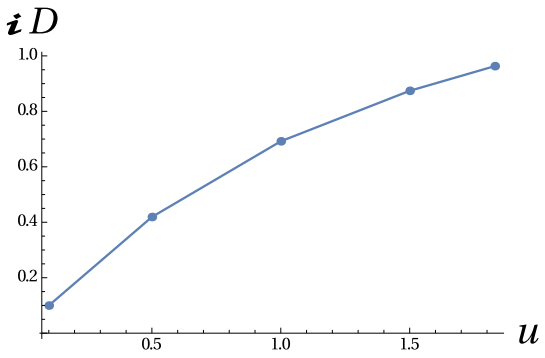

Figure 4.6: iD vs the deformation parameter u at $L = 4.5$.

$A_1 = \pi/L$. Moreover, the same reason ensures that although the Lüscher term in (4.4.5) comes from fermions it still gives negative contribution to the energy as compared to the non-supersymmetric case.

The vacuum energy (4.4.5) can be compared to the vacuum energy in the Z_{2N} broken phase below the curve (4.4.2) in the limit of $Lm_f \ll 1$,

$$E \approx \frac{LN\Lambda^2}{4\pi}\left(1 + \frac{2}{\Lambda L}\sqrt{\frac{8\pi}{\Lambda L}}e^{-\Lambda L}\right) - \frac{\pi N}{6L} - \frac{NS_2}{4\pi L}(Lm_f)^4 \,. \tag{4.4.6}$$

The energy difference is approximately given by the last term above. Equation (4.4.1) tells us that the energy difference behaves as $\sim (L - L_c(u))^2$ near the phase transition

curve, where $L_c(u)$ is given by (4.4.2).

In summary, we conclude that as we increase u and cross the curve (4.4.2) our system goes through a line of *third* order phase transitions into the phase with $\sigma = 0$. All N vacua coalesce in the σ plane and Z_{2N} symmetry is restored. In the infrared limit our theory in this phase flows to a conformal limit which is a free theory of massless fermions ξ^l.

4.4.2 What happens with the A_μ auxiliary field in the Z_{2N} unbroken phase

As we move into the Z_{2N} unbroken phase by increasing u we could, in principle, observe two distinct scenarios: the N former vacua of the Z_{2N} broken phase which fuse themselves into $\sigma = 0$ in phase III, in fact, split in energy, with $N-1$ of them becoming quasivacua, and only one of them remaining as the true vacuum. This phase would be quite similar to the Coulomb/confinement phase in the non-supersymmetric CP($N-1$) model described in Chapter 3 (see also [26]).

The second option is to have just a unique vacuum at $\sigma = 0$, with no accompanying family of quasivacua. One can decide between the two options by analyzing the auxiliary field A_μ.

We need to evaluate the two diagrams shown in Fig. (4.7). The first diagram

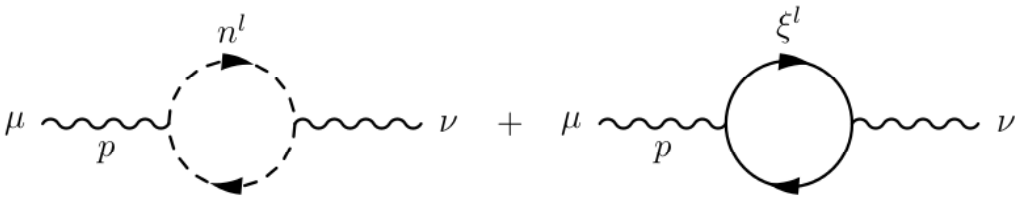

Figure 4.7: One loop diagrams that contribute to the photon kinetic term.

comes from bosons n^l. In much the same way as in the non-supersymmetric CP($N-1$) model it produces a kinetic term for the photon in the Lagrangian,

$$\frac{1}{4e^2} F_{kl}^2 \,, \tag{4.4.7}$$

where at large L the expression for the charge e^2 is given by

$$\frac{1}{e^2} \approx \frac{N}{12\pi\Lambda^2}\,. \tag{4.4.8}$$

This makes U(1) gauge field dynamical [26]. In the non-supersymmetric model this leads to confinement of electric charges. The reason is that the static Coulomb potential in two dimensions is linear and ensures that the charged n^l states are linearly confined in the non-supersymmetric model [26]. Similar Coulomb/confining phase occurs in the compactified non-supersymmetric CP($N-1$) model at large L (see Chapter 3). Confinement of n^l states can be interpreted as a small split between quasivacua involved in the θ-angle evolution [35, 18]. In this picture the n^l states are interpreted as kinks interpolating between true vacuum an the first quasivacuum.

On the other hand, in our $\mathcal{N}=(0,2)$ theory we have also the second diagram coming from massless fermions. It produces a mass term for the photon

$$V(A_1) = \frac{N}{2\pi}\left(A_1 - \frac{\pi}{L}\right)^2\,. \tag{4.4.9}$$

Evaluation of the coefficient $N/2\pi$ is presented in Appendix E. This term is a manifestation of the chiral anomaly and appears in much the same way as in the Schwinger model.

Therefore, the photon obtains a mass

$$m_\gamma \approx \sqrt{12}\Lambda\,. \tag{4.4.10}$$

The photon mass ensures the exponential fall-off of the electric potential between charged sources. Thus, there is no confinement in the $\sigma = 0$ phase of our (0,2) supersymmetric CP($N-1$) model.

This ensures the absence of fine vacuum structure with split quasivacua. In fact there is no θ dependence in the theory with massless fermions, and the argument of [35] does not apply. We have a single vacuum with the unbroken Z_{2N} symmetry and no family of quasivacua in the $\sigma = 0$ phase (i.e. phase III in Fig. 1). This is a new phase in the CP($N-1$) model which was not known before.

4.5 Would be broken SU(N) phase

Now let us consider the region of small L. At small L the theory enters a weak coupling regime so we expect the emergence of the classical picture in the limit $N \to \infty$. Classically CP($N-1$) model has $2(N-1)$ massless states which can be viewed as Goldstone states of the broken SU(N) symmetry. To study this possibility much in the same way as in [44] we assume that one component of the field n^l, say $n^1 \equiv n$ can develop VEV and we integrate over all other components of n^l in the external fields n, σ D and A_1. However now in order not to break supersymmetry by the boundary conditions we have to leave out one component of ξ fields as well. Due to the constraint (4.1.5) we can choose these components to be $\xi^N_{L,R} \equiv \xi_{L,R}$. The expression for the energy is

$$\begin{aligned} E &= \frac{LN}{4\pi}\Bigg[iD - iD\ln\frac{m_b^2}{\Lambda^2} - m_f^2\ln\frac{m_b^2}{m_f^2} + m_f^2 u \\ &+ 8m_f^2\sum_{k=1}^{\infty}\frac{K_1(Lm_f k)}{Lm_f k}\cos(kLA_1) - 8m_b^2\sum_{k=1}^{\infty}\frac{K_1(Lm_b k)}{Lm_b k}\cos(kLA_1)\Bigg] \\ &+ L\left[(m_b^2 + A_1^2)|n|^2 + i\sqrt{2}\sigma\bar{\xi}_R\xi_L + i\sqrt{2}\sigma^\star\bar{\xi}_L\xi_R\right] \\ &+ i\bar{\xi}_L\xi_L LA_1 - i\bar{\xi}_R\xi_R LA_1 \\ &+ N\left[\sqrt{m_f^2 + A_1^2} - \sqrt{m_b^2 + A_1^2}\right], \end{aligned} \tag{4.5.1}$$

where the first two lines are the same as in (4.2.1), the third and fourth lines correspond to components which we left out of integration, and the last line gives the contribution due to omission of the zero modes.

4.5.1 Saddle point approximation

Proceeding as in the SU(N) symmetric case we obtain the following set equations that defines a stationary point

$$0 = (m_b^2 + A_1^2)n\,, \tag{4.5.2}$$

$$0 = \sqrt{2}\sigma\xi_L - \xi_R A_1 = \sigma^\star\xi_R + \xi_L A_1\,, \tag{4.5.3}$$

$$|n|^2 = \frac{N}{L}\Big[\frac{1}{2\sqrt{m_b^2 + A_1^2}} + \frac{L}{4\pi}\ln\frac{m_b^2}{\Lambda^2} - \frac{L}{\pi}\sum_{k=1}^{\infty} K_0(Lm_b k)\cos(kLA_1)\Big], \tag{4.5.4}$$

$$\begin{aligned} 0 = {} & N\Big[\frac{2Lm_b}{\pi}\sum_{k=1}^{\infty} K_1(Lm_b k)\sin(kLA_1) - \frac{2Lm_f}{\pi}\sum_{k=1}^{\infty} K_1(Lm_f k)\sin(kLA_1), \\ & - \frac{A_1}{\sqrt{m_b^2 + A_1^2}} + \frac{A_1}{\sqrt{m_f^2 + A_1^2}}\Big] + 2LA_1|n|^2 + iL\bar{\xi}_L\xi_L - iL\bar{\xi}_R\xi_R \end{aligned} \tag{4.5.5}$$

$$\begin{aligned} 0 = {} & Li\sqrt{2}\bar{\xi}_L\xi_R + 2\sigma\Big[L|n|^2 + N\Big(-\frac{1}{2\sqrt{m_b^2 + A_1^2}} + \frac{1}{2\sqrt{m_f^2 + A_1^2}} \\ & + \frac{L}{\pi}\sum_{k=1}^{\infty} K_0(Lm_b k)\cos(kLA_1) - \frac{L}{\pi}\sum_{k=1}^{\infty} K_0(Lm_f k)\cos(kLA_1)\Big), \\ & + \frac{LN}{4\pi}\Big(u - \ln\frac{m_b^2}{m_f^2}\Big)\Big]\,. \end{aligned} \tag{4.5.6}$$

From (4.5.2) we conclude that $m_b = A_1 = 0$. Then (4.5.5) does not have a solution unless $\sigma = 0$. We also see that $\bar{\xi}_{L,R} = \xi_{L,R} = 0$ satisfies the above system of equations. We find that n^l field develops a vacuum expectation value

$$|n|^2 = \frac{N}{2\pi}\left(\ln\frac{4\pi}{\Lambda L} - \gamma\right)\,, \tag{4.5.7}$$

which implies in turn that this solution exists only for $\Lambda L \leq 7.05$. The energy is found to be zero as in the supersymmetric case, see phase I in Fig. (1).

This phase is similar to the dynamical regime we found previously in the non-supersymmetric CP($N-1$) model in Chapter (3). In particular, the VEV of n^l breaks global SU(N) symmetry implying the presence of $2(N-1)$ real massless degrees of freedom. As we already mentioned the dynamics of the CP($N-1$) model in this phase

is determined by quasiclassical approximation in the action (4.1.1). At small L the theory is at weak coupling because the inverse coupling constant r is determined by

$$r = \frac{N}{2\pi} \log \frac{1}{L\Lambda}. \tag{4.5.8}$$

The constant r grows large at small L.

However, we do not expect exactly massless modes to appear in $1+1$ dimensions because of Mermin-Wagner-Coleman's theorem [51, 39]. We found the above solution in the leading order in $1/N$. It holds only in the limit $N = \infty$. Thus, we should expect higher order corrections to modify the result. In particular, the would-be Goldstone massless modes may acquire small masses suppressed in the large N limit. As a consequence the energy might be uplifted from zero.

The solution that we found is completely u-independent. Thus we expect that the vacuum energy in the would be broken phase is given by E_{br} which is independent on u and suppressed at large N.

4.6 Quantum mechanics at small L: $u \to 0$ limit

Now we have to study the limit $u \to 0$ at small L where the theory should match the $\mathcal{N} = (2,2)$ CP$(N-1)$ model which has a single SU(N) symmetric (Z_{2N} broken) phase with the mass gap independent of L. Clearly the would be broken SU(N) phase cannot explain this limit because it is u-independent. Our analysis in this section has a qualitative nature. As we have already seen, for the case of large L the transition occurs at $uN^2 \sim 1$ where the large-N approximation strictly speaking is not applicable.

Below we argue that the SU(N) symmetric phase reappear again when we go to the limit of extremely small u keeping L small, $L \ll 1/\Lambda$. Assuming that both $Lm_{b,f} \ll 1$ in this phase we use (D.13) to find the expression for the potential valid for LA_1 close to π

$$V(\tilde{A}_1) \approx \frac{NL^2}{\pi} \tilde{A}_1^2 \left(m_b^2 - m_f^2\right) S_2\,, \tag{4.6.1}$$

where $\tilde{A}_1 \equiv A_1 - \pi/L$. By analogy with (4.4.1) one can find the expression for the bosonic mass

$$(Lm_b)^2 S_2 \approx S_1 + \gamma - \ln \frac{4\pi}{\Lambda L}\,. \tag{4.6.2}$$

Thus the expression for the potential is given by

$$V(\tilde{A}_1) \approx \frac{Nu}{2\pi}\tilde{A}_1^2\,, \tag{4.6.3}$$

Hence, as u gets smaller the potential becomes weaker and flatter. When LA_1 gets close to 0 or 2π the above expression becomes invalid. The results of numerical calculations are given in Fig. (4.8). Two curves correspond to two values of deformation parameter $u = 0.05$ and $u = 0.1$ (dashed curve). One can see that the expression we derived is in a good agreement with numerical results. As u gets smaller the amplitude of the potential also decreases.

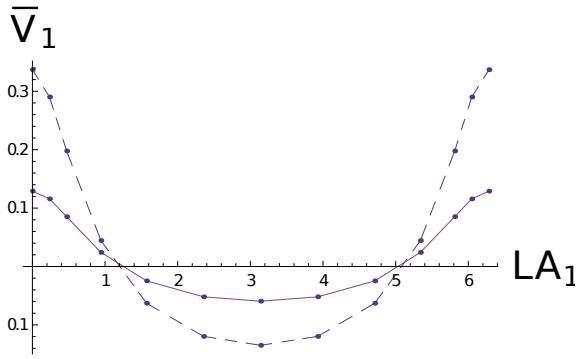

Figure 4.8: Dependence of potential $\bar{V}_1 \equiv \dfrac{\pi L^2}{2N}V$ on the deformation parameter u.

We see that in the limit $u \to 0$ the potential $V(\tilde{A}_1)$ becomes flat and we have to average over A_1 (instead of taking the saddle point value $A_1 = \pi/L$) in much the similar way as we did in Sec. 4.3.1 for the region of large L. The averaging procedure gives us $\mathcal{N} = (2, 2)$ limit.

More exactly the vacuum energy in SU(N) symmetric phase at extremely small u is given by

$$E_{sym} \approx \frac{uN}{4\pi}\Lambda^2\, L\,. \tag{4.6.4}$$

Comparing this with the vacuum energy E_{br} in the would be broken SU(N) phase which is independent of u we see that at very small critical $u_c \sim 1/N^2$, the energy in the SU(N) unbroken phase becomes lower then that in the SU(N) broken phase, and

the system undergoes a phase transition into SU(N) symmetric phase, see Fig. 1. The SU(N) symmetric phase has a perfectly smooth $u \to 0$ limit.

Chapter 5

Conclusion and Discussion

In Chapter 2 we discussed the theory supporting strings with extra (rotational) moduli on the string world sheet. Our numerical analysis demonstrates that it is not difficult to endow the ANO string with such moduli following a strategy similar to that used by Witten in constructing cosmic strings. Our discussion was carried out in the quasiclassical approximation.

When the bulk model is deformed by a spin-orbit interaction a number of entangled terms emerge on the string world sheet. Quantum effects on the string world sheet (which can be made arbitrarily small with a judicious choice of parameters) is a subject of a separate study.

We also found numerical solutions for the profile functions and calculated the tensions of two distinct (but degenerate) strings. This proves the possibility of coexistence of the ANO and non-Abelian degenerate strings in one and the same model simultaneously. The classical degeneracy is not protected against quantum corrections. The obvious next step is to supersymmetrize the model to see whether or not one can have the two strings BPS-saturated. Then the degeneracy will be preserved in higher orders. Another interesting project is to slightly change the parameters of the model to make the two strings slightly non-degenerate, with the aim of calculating the decay rate of the heavier string into the lighter one.

In Chapter 3 we studied two-dimensional CP($N-1$) model (both nonsupersymmetric and $\mathcal{N} = (2,2)$) compactified on a cylinder with circumference L (periodic boundary conditions). We found the large-N solution for any value of L and discussed in detail

the large-L and small-L limits.

A drastic difference is detected in passing from the nonsupersymmetric to $\mathcal{N} = (2, 2)$ supersymmetric case. In the former case in the large-N limit we observe a phase transition at $L \sim \Lambda_{\rm CP}^{-1}$ (which is expected to become a rapid crossover at finite N). At large L the CP($N-1$) model develops a mass gap and is in the Coulomb/confinement phase, with exponentially suppressed finite-L effects. At small L it is in the deconfinement phase; the orientational modes contribute to the Lüsher term. The latter becomes dependent on the rank of the bulk gauge group.

In the supersymmetric CP($N-1$) model we have a different picture. Our large-N solution exhibits a single phase independently of the value of $L\Lambda_{\rm CP}$. For any value of this parameter a mass gap develops and supersymmetry remains unbroken. So does the $SU(N)$ symmetry of the target space (i.e. it is restored). The mass gap turns out to be independent of the string length. The Lüscher term is absent due to supersymmetry.

In Chapter 4 we studied heterotic $\mathcal{N} = (0, 2)$ CP($N-1$) model and found three different phases, see Fig. 1. At large L and intermediate values of the deformation parameter u there is a phase (IV) with a mass gap, N vacua and broken discrete Z_{2N} symmetry. As we increase u a reach a critical value (which grows with L) we find a phase transition to the Z_{2N} symmetric phase (III), with a unique vacuum. The line separating these two SU(N) symmetric phases is a line of a third order phase transitions in the large N limit.

As the string under consideration gets shorter we find a phase transition to a phase with the would be broken SU(N) symmetry (phase II). In this phase we expect masses of the n fields to be much smaller than in two SU(N) symmetric phases. In fact, at $N = \infty$ they vanish. At small L and extremely small u we expect another phase transition from the would be broken SU(N) phase into the SU(N) unbroken phase (I) which has a smooth $u \to 0$ limit.

Strictly speaking, our description of the underlying dynamics in terms of the phase transitions is valid only at $N = \infty$. At large but finite N one can expect that all phase transitions become rapid crossovers.

References

[1] A. Abrikosov, Sov. Phys. JETP **32**, 1442 (1957) [Reprinted in *Solitons and Particles*, Eds. C. Rebbi and G. Soliani (World Scientific, Singapore, 1984), p. 356]; H. Nielsen and P. Olesen, Nucl. Phys. **B61**, 45 (1973) [Reprinted in *Solitons and Particles*, Eds. C. Rebbi and G. Soliani (World Scientific, Singapore, 1984), p. 365].

[2] G. t Hooft, *Topology of the gauge condition and new confinement phases in non-Abelian gauge theories*, 1981NuPhB.190..455T; S. Mandelstam, *Vortices and quark confinement in non-Abelian gauge theories* Phys. Rept. 23, 245 (1976)

[3] N. Seiberg, E. Witten, *Electric-magnetic duality, monopole condensation, and confinement in $\mathcal{N} = 2$ supersymmetric Yang-Mills theory*, Nucl. Phys. B 426, 19 (1994), (E) B 430, 485 (1994) [hep-th/9407087]; *Monopoles, duality and chiral symmetry breaking in $\mathcal{N} = 2$ supersymmetric QCD,* Nucl. Phys. B 431, 484 (1994) [hep-th/9408099].

[4] A. Hanany and D. Tong, *Vortices, Instantons and Branes,* JHEP **0307**, 037 (2003) [hep-th/0306150].

[5] R. Auzzi, S. Bolognesi, J. Evslin, K. Konishi and A. Yung, *Non-Abelian superconductors: Vortices and confinement in $N = 2$ SQCD,* Nucl. Phys. B **673**, 187 (2003) [hep-th/0307287].

[6] M. Shifman and A. Yung, *Non-Abelian string junctions as confined monopoles,* Phys. Rev. D **70**, 045004 (2004) [hep-th/0403149].

[7] A. Hanany and D. Tong, *Vortex Strings and Four-Dimensional Gauge Dynamics,* JHEP **0404**, 066 (2004) [hep-th/0403158].

[8] D. Tong, *TASI Lectures on Solitons,* arXiv:hep-th/0509216.

[9] M. Eto, Y. Isozumi, M. Nitta, K. Ohashi and N. Sakai, *Solitons in the Higgs phase: The moduli matrix approach,* J. Phys. A **39**, R315 (2006) [arXiv:hep-th/0602170].

[10] M. Shifman and A. Yung, *Supersymmetric Solitons,* Rev. Mod. Phys. **79** 1139 (2007) [arXiv:hep-th/0703267]; an expanded version in Cambridge University Press, 2009.

[11] D. Tong, *Quantum Vortex Strings: A Review,* Annals Phys. **324**, 30 (2009) [arXiv:0809.5060 [hep-th]].

[12] G. Volovik, *The Universe in a Helium Droplet*, (Oxford University Press, 2003); A. J. Leggett, *Quantum Liquids* (Oxford University Press, 2006).

[13] M. Nitta, M. Shifman and W. Vinci, *On Non-Abelian Quasi-Gapless Modes Localized on Mass Vortices in Superfluid 3He-B,* Phys. Rev. D **87**, 081702 (2013) [arXiv:1301.3544 [cond-mat.other]].

[14] M. Shifman, *Simple Models with Non-Abelian Moduli on Topological Defects,* Phys. Rev. D **87**, 025025 (2013) [arXiv:1212.4823 [hep-th]].

[15] M. Shifman and A. Yung, Phys. Rev. Lett. **110**, 201602 (2013) [arXiv:1303.7010 [hep-th]].

[16] E. A. Ivanov and V. I. Ogievetsky, *The Inverse Higgs Phenomenon in Nonlinear Realizations,* Teor. Mat. Fiz. **25**, 164 (1975) [English version in JINR Report JINR-E2-8593].

[17] I. Low and A. V. Manohar, *Spontaneously broken space-time symmetries and Goldstone's theorem,* Phys. Rev. Lett. **88**, 101602 (2002) [hep-th/0110285].

[18] A. Gorsky, M. Shifman, A. Yung, *Non-Abelian Meissner effect in Yang-Mills theories at weak coupling,* Phys. Rev. D 71, 045010 (2005) [arXiv:hep-th/0412082].

[19] M. Teper, *Large-N and confning flux tubes as strings - a view from the lattice*, Acta Phys. Polon. B **40**, 3249 (2009) [arXiv:0912.3339].

[20] A. Athenodorou and M. Teper, *Closed flux tubes in D=2+1 SU(N) gauge theories: dynamics and effective string description,* arXiv:1602.07634 [hep-lat].

[21] O. Aharony and Z. Komargodski, *The effective theory of long strings* JHEP **1305**, 118 (2013) [arXiv:1302.6257].

[22] S. Dubovsky, R. Flauger, and V. Gorbenko, *Effective String Theory Revisited*, JHEP **1209**, 044 (2012), [arXiv:1203.1054].

[23] A. Athenodorou, B Bringoltz, M. Teper *Closed Flux Tubes and Their String Description in D=3+1 SU(N) Gauge Theories,* JHEP **1102**, 030 (2011) [arXiv:1007.4720 [hep-lat]].

[24] M. Lüscher, *Symmetry Breaking Aspects of the Roughening Transition in Gauge Theories,* Nucl. Phys. B **180**, 317 (1981).

[25] M. Shifman and A. Yung, *Non-Abelian strings and the Lüscher term,* Phys. Rev. D **77**, 066008 (2008) [arXiv:0712.3512 [hep-th]].

[26] E. Witten, *Instantons, the Quark Model, and the 1/N Expansion,* Nucl. Phys. B **149**, 285 (1979).

[27] M. Shifman, A. Yung, *Non-Abelian Flux Tubes in SQCD: Supersizing World-Sheet Supersymmetry*, Phys. Rev. D 72, 085017 (2005) [arXiv:hep-th/0501211]

[28] M. Edalati, D. Tong, *Heterotic Vortex Strings*, JHEP 0705, 005 (2007) [arXiv:hep-th/0703045].

[29] M. Shifman and A. Yung, *Heterotic Flux Tubes in N=2 SQCD with N=1 Preserving Deformations,* Phys. Rev. D **77**, 125016 (2008) [arXiv:0803.0158 [hep-th]].

[30] J. Chen, X. Cui, M. Shifman and A. Vainshtein, *On Isometry Anomalies in Minimal* $\mathcal{N} = (0,1)$ *and* $\mathcal{N} = (0,2)$ *Sigma Models,* arXiv:1510.04324 [hep-th].

[31] E. Witten, *Superconducting Strings,* Nucl. Phys. B **249**, 557 (1985).

[32] M. Shifman, *Advanced Topics in Quantum Field Theory*, (Cambridge University Press, 2012).

[33] E. B. Bogomol'nyi, *Sov. J. Nucl. Phys.* **24**, 449 (1976), reprinted in *Solitons and Particles*, eds. C. Rebbi and G. Soliani (World Scientific, Singapore, 1984) p. 389. M. K. Prasad and C. M. Sommerfield, *Phys. Rev. Lett.* **35**, 760 (1975), reprinted in *Solitons and Particles*, Eds. C. Rebbi and G. Soliani (World Scientific, Singapore, 1984) p. 530.

[34] K. Bardakci, M.B. Halpern, *Spontaneous Breakdown and Hadronic Symmetries,* Phys. Rev. D 6, 696 (1972)

[35] E. Witten, *Theta dependence in the large-N limit of four-dimensional gauge theories,* Phys. Rev. Lett. **81**, 2862 (1998), [hep-th/9807109].

[36] I. Affleck, *The Role of Instantons in Scale Invariant Gauge Theories,* Nucl. Phys. B **162**, 461 (1980).

[37] G. Lazarides, *The Effect of Statistical Fluctuations on Confinement and on the Vacuum Structure of the* $CP^{(n-1)}$ *Models,* Nucl. Phys. B **156**, 29 (1979).

[38] A. Actor, *Temperature Dependence of CP^{N-1} Model and the Analogy with Quantum Chromodynamics,* Fortschr. Phys. **33**, 333 (1985).

[39] S. R. Coleman, *There are no Goldstone bosons in two-dimensions,* Commun. Math. Phys. **31**, 259 (1973).

[40] S. W. Hawking, *Zeta Function Regularization of Path Integrals in Curved Spacetime,* Commun. Math. Phys. 55, 133 (1977).

[41] A. Milekhin, *CP(N-1) model on finite interval in the large N limit,* Phys. Rev. D **86**, 105002 (2012) [arXiv:1207.0417 [hep-th]].

[42] I. S. Gradshteyn, I. M. Ryzhik, *Table of Integrals, Series, and Products*, (Academic Press, New York, 1980).

[43] M. Abramowitz, I. Stegun, *Handbook of Mathematical Functions: with Formulas, Graphs, and Mathematical Tables.*

[44] A. Gorsky, M. Shifman and A. Yung, *The Higgs and Coulomb/Confining Phases in "Twisted-Mass" Deformed CP(N-1) Model,* Phys. Rev. **D73**, 065011 (2006) [arXiv:hep-th/0512153].

[45] G. V. Dunne and M. Ünsal, *Resurgence and Trans-series in Quantum Field Theory: The CP(N-1) Model,* JHEP **1211**, 170 (2012) [arXiv:1210.2423 [hep-th]].

[46] M. Shifman, Alexei Yung, *Large-N Solution of the Heterotic $\mathcal{N} = (0, 2)$ Two-Dimensional $CP(N-1)$ Model*, Phys. Rev. D 77, 125017 (2010) [arXiv:0803.0698]

[47] A. D'Adda, A. C. Davis, P. DiVeccia and P. Salamonson, *An effective action for the supersymmetric CP^{n-1} models,* Nucl. Phys. **B222** 45 (1983).

[48] E. Witten, *Phases of $N = 2$ theories in two dimensions,* Nucl. Phys. B **403**, 159 (1993) [hep-th/9301042].

[49] S. Cecotti and C. Vafa, *On classification of $\mathcal{N} = 2$ supersymmetric theories,* Comm. Math. Phys. **158** 569 (1993).

[50] D.Tong, C. Turner, *Quantum dynamics of supergravity on $R^3 \times S^1$*, JHEP 1412 (2014) 142, [arXiv:1408.3418]

[51] N.D. Mermin and H. Wagner, *Absence of Ferromagnetism or Antiferromagnetism in One- or Two-Dimensional Isotropic Heisenberg Models,* Phys. Rev. Lett. **17**, 1133 (1966).

[52] E.T. Whittaker, G.N. Watson, *A course of modern analysis* (1927).

Appendix A

Calculation of Zeta function

We define the zeta function of an operator Ω as follows:

$$\zeta(s) = Tr\ \Omega^{-s}\,. \tag{A.1}$$

The operator of interest is given in Eq. (3.2.3),

$$\Omega = -(\partial_k - iA_k)^2 + m^2\,, \tag{A.2}$$

where instead of ω we write m^2. In the $A_1 = 0$ gauge the expression for the zeta function takes the form

$$\zeta(s) = \frac{\hat{T}}{2\pi}\sum_{k=-\infty}^{\infty}\int_{-\infty}^{\infty} dq_1 \left(q_1^2 + \left(\frac{2\pi k}{L} + A_0\right)^2 + m^2\right)^{-s}\,. \tag{A.3}$$

Gauge invariance requires invariance under transformation $A_0 \to A_0 + 2\pi k_0/L$, where k_0 is integer. This is manifest in (A.3) since the shift can be absorbed in the sum. We always can look for a solution for A_0 in the interval $|A_0| < \pi/L$, say $A_0 = 0$.

To evaluate the expression in (A.3) we will need the following identities

$$\Gamma(Z) = \int_0^\infty dt\, t^{z-1}\, e^{-t}\,, \tag{A.4}$$

$$\int_0^\infty dx (x^2)^{(\alpha-1)/2}(x^2 + A^2)^{\beta-1} = \frac{1}{2}(A^2)^{\beta-1+\alpha/2} B(\alpha/2, 1-\beta-\alpha/2)\,,$$

$$B(x,y) = \frac{\Gamma(x)\Gamma(y)}{\Gamma(x+y)}\,. \tag{A.5}$$

The definition of the modified Bessel functions of second kind is

$$\int_0^\infty dx\, x^{\nu-1} \exp\left(-\frac{a}{x} - bx\right) = 2\left(\frac{a}{b}\right)^{\nu/2} K_\nu\left(2\sqrt{ab}\right) . \tag{A.6}$$

The definition of the theta function (see Chapter 21 of [52]) is

$$\Theta_3(x,\tau) = \sum_{k=-\infty}^{\infty} q^{k^2}\, e^{2\pi i x} = 1 + 2\sum_{k=1}^{\infty} q^{k^2} \cos 2kx\,, \quad q = e^{\pi i \tau}\,, \tag{A.7}$$

Its Jacobi transformation is

$$\Theta_3(x,\tau) = (-i\tau)^{-1/2} \exp\left(\frac{x^2}{i\pi\tau}\right) \Theta_3(x/\tau, -1/\tau)\,. \tag{A.8}$$

The evaluation of the zeta function, Eq. (A.3), proceeds as follows:

$$\begin{aligned}
\zeta(s) &\overset{(A.5)}{=} \frac{\hat{T}}{2\pi}\frac{\Gamma(\frac{1}{2})\Gamma(s-\frac{1}{2})}{\Gamma(s)} \sum_{k=-\infty}^{\infty}\left[\left(\frac{2\pi k}{L} + A_0\right)^2 + m^2\right]^{1/2-s} \\
&= \frac{\hat{T}}{2\pi}\frac{\Gamma(\frac{1}{2})\Gamma(s-\frac{1}{2})}{\Gamma(s)} \left(\frac{2\pi}{L}\right)^{1-2s} \sum_{k=-\infty}^{\infty}\left[\left(k + \frac{LA_0}{2\pi}\right)^2 + \epsilon^2\right]^{1/2-s} \\
&\overset{(A.4)}{=} \frac{\hat{T}}{2\pi}\frac{\Gamma(\frac{1}{2})\Gamma(s-\frac{1}{2})}{\Gamma(s)} \left(\frac{2\pi}{L}\right)^{1-2s} \frac{1}{\Gamma(z)} \\
&\times \int_0^\infty dt\, t^{z-1} e^{-t\alpha^2} \sum_{k=-\infty}^{\infty} e^{-k^2 t - k\beta^2 t} \\
&\overset{(A.7)}{=} \frac{\hat{T}}{2\pi}\frac{\Gamma(\frac{1}{2})\Gamma(s-\frac{1}{2})}{\Gamma(s)} \left(\frac{2\pi}{L}\right)^{1-2s} \frac{1}{\Gamma(z)} \\
&\times \int_0^\infty dt\, t^{z-1} e^{-t\alpha^2} \Theta_3\left(\frac{i\beta^2 t}{2}, \frac{it}{\pi}\right) \\
&\overset{(A.8),(A.7)}{=} F\frac{\sqrt{\pi}}{\Gamma(z)} \int_0^\infty dt\, t^{z-3/2} e^{-t\alpha^2 + \beta^4 t/4} \left(1 + 2\sum_{k=1}^{\infty} e^{-\frac{k^2\pi^2}{t}} \cos \pi k\beta^2\right) \\
&\overset{(A.6)}{=} F\frac{\sqrt{\pi}}{\Gamma(z)} \left(\frac{1}{G^2}\right)^{z-\frac{1}{2}}
\end{aligned}$$

$$\times \quad \left(\Gamma(z-\frac{1}{2})+4\sum_{k=1}^{\infty}(\pi kG)^{z-\frac{1}{2}}K_{z-\frac{1}{2}}(2\pi kG)\cos\pi k\beta^2\right)$$

$$\stackrel{(A.6)}{=} \quad \frac{\hat{T}L}{4\pi}\frac{1}{m^{2s-2}}\left[\frac{1}{s-1}\right.$$

$$+ \quad \left.\frac{4}{\Gamma(s)}\sum_{k=1}^{\infty}\left(\frac{Lmk}{2}\right)^{s-1}K_{s-1}(Lmk)\cos LA_0k\right], \tag{A.9}$$

where we introduced intermediate notations

$$\epsilon=\frac{Lm}{2\pi}, \quad z=s-\frac{1}{2}, \quad F=\frac{\hat{T}}{2\pi}\frac{\Gamma(\frac{1}{2})\Gamma(s-\frac{1}{2})}{\Gamma(s)}\left(\frac{2\pi}{L}\right)^{1-2s}, \tag{A.10}$$

and

$$\alpha^2=\left(\frac{LA_0}{2\pi}\right)^2+\left(\frac{Lm}{2\pi}\right)^2, \quad \beta^2=\frac{LA_0}{\pi}, \quad G^2=\alpha^2-\beta^4/4\,. \tag{A.11}$$

To find the derivative of the zeta function we will make use of the following properties of Euler's Γ function:

$$\Gamma(z+1)=z\Gamma(z), \quad \Gamma(0)=\infty\,. \tag{A.12}$$

The derivative is evaluated as follows:

$$\begin{aligned}\zeta'(s) &= \frac{\hat{T}L}{4\pi}\left[-\frac{1}{m^{2s-2}}\frac{1}{(s-1)^2}-\frac{2\ln m}{m^{2s-2}(s-1)}\right.\\ &\quad \left.-\frac{4\Gamma'(s)}{\Gamma^2(s)m^{2s-2}}\sum_{n=1}^{\infty}\left(\frac{Lmk}{2}\right)^{s-1}K_{s-1}(Lmk)\cos LA_0k\right]\Bigg|_{s=0}\\ &= \frac{\hat{T}Lm^2}{4\pi}\left[-1+\ln m^2+8\sum_{k=1}^{\infty}\frac{K_1(kLm)}{kLm}\cos LA_0k\right]\end{aligned} \tag{A.13}$$

Following [40] we can write the generating functional,

$$\ln Z=\frac{1}{2}\zeta'(0)+\frac{1}{2}\ln\mu^2\zeta(0)\,, \tag{A.14}$$

where a normalization constant μ has dimension of mass. Renormalizability requires

$$\mu=M_{\rm uv}\,.$$

Thus, in terms of the zeta function and its derivative the expression for the effective potential becomes

$$V = -\frac{N}{\hat{T}}\left(\zeta'(0) + \zeta(0)\ln M_{uv}^2\right) - \frac{N}{4\pi}Lm^2\ln\frac{M_{\rm uv}^2}{\Lambda^2}\,. \tag{A.15}$$

Substituting the expressions for the zeta function and its derivative we obtain

$$V = \frac{NL\omega}{4\pi}\left[1 - \ln\frac{\omega}{\Lambda_{CP}^2} - 8\sum_{k=1}^{\infty}\frac{K_1(kL\sqrt{\omega})}{kL\sqrt{\omega}}\cos kLA_0\right]\,, \tag{A.16}$$

where we replaced m^2 by ω.

Appendix B

Kinetic term in case of bosonic theory

To find the U(1) charge of the n^l fields one has to consider only the second diagram in Fig. (3.1). The first diagram is needed only for renormalization. The relevant part of the action written in the Minkowski spacetime takes the form

$$\begin{aligned} iS_B^M &= i\int d^2x \left[\nabla_\mu \bar{n}_l \nabla^\mu n^l - m^2|n|^2\right] \\ &= i\int d^2x \left[\partial_\mu \bar{n}_l \partial^\mu n_l - m^2|n|^2 + iA^\mu(\bar{n}_l \overleftrightarrow{\partial}_\mu n^l) + A^2|n|^2\right], \end{aligned} \tag{B.1}$$

where $\overleftrightarrow{\partial}_\mu = \overrightarrow{\partial}_\mu - \overleftarrow{\partial}_\mu$. We then pass to Euclidean space,

$$t = -i\tau\,, \quad A_0 = i\hat{A}_0\,, \quad A_i = \hat{A}_i\,.$$

The action in Euclidean space is

$$S_B^E = \int d^2\hat{x} \left[\partial_k \bar{n}_l \partial_k n_l + m^2|n|^2 + i\hat{A}_k(\bar{n}_l \overleftrightarrow{\partial}_k n^l) + \hat{A}^2|n|^2\right]. \tag{B.2}$$

Now we can determine the Feynman rules. The results are shown in Fig. (B.1). Thus for the kinetic term (in the case of an infinitely long string) one can write

$$\Pi_{ij} = N\int \frac{d^2q}{(2\pi)^2} \frac{(p_i+2q_i)(p_j+2q_j)}{(m^2+q^2)(m^2+(p+q)^2)}\,. \tag{B.3}$$

Introducing the Feynman parameter to combine the denominators

$$\frac{1}{\alpha(\alpha+\beta)} = \int_0^1 dx\, \frac{1}{(x\beta+\alpha)^2}\,, \tag{B.4}$$

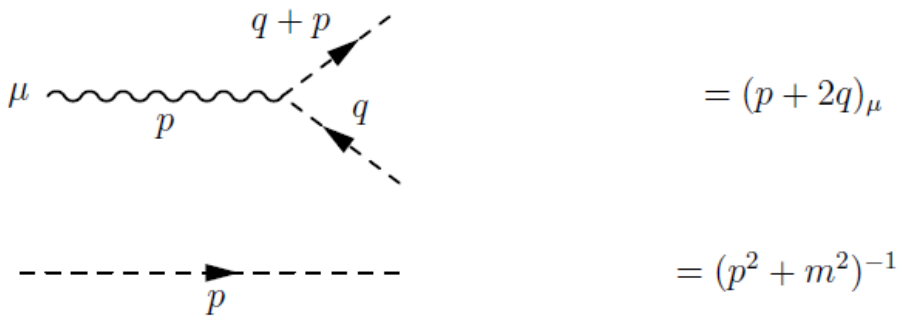

Figure B.1: Feynman rules: vertex and the propagator of n^l field.

and substituting $l = q + px$ in Eq. (B.3) we arrive at

$$\Pi_{ij} = N \int \frac{d^2l\, dx}{(2\pi)^2} \frac{\left[p_i p_j (1-2x)^2 - 2x(p_i l_j + p_j l_i) + 4 l_i l_j\right]}{(l^2 + m^2 + p^2 x(1-x))^2} \,. \tag{B.5}$$

Terms linear in l vanish. To find the U(1) charge we only need to consider the $p_i p_j$ structure. Thus, the expression for the charge is

$$\frac{1}{Ne^2} = \int \frac{d^2l\, dx}{(2\pi)^2} \frac{(1-2x)^2}{(l^2 + m^2 + p^2 x(1-x))^2} = \int_0^1 \frac{dx}{4\pi} \frac{(1-2x)^2}{m^2 + p^2 x(1-x)} \,. \tag{B.6}$$

Expanding the last expression to the zeroth power in p one finally finds

$$\frac{1}{Ne^2} = \int_0^1 \frac{dx}{4\pi m^2} (1-2x)^2 = \frac{1}{12\pi m^2} \,. \tag{B.7}$$

The case of the finite length string is considered along similar lines. We recall (see [36]) that the limit $p_\mu \to 0$ is understood as first putting $p_0 = 0$ and then letting p_1 go continuously to zero. As a result, only $\Pi_{00} \neq 0$. Using the Feynman rules one can derive the following expression:

$$\Pi_{00} = \frac{N}{L} \sum_{k=-\infty}^{\infty} \int \frac{dq}{2\pi} \frac{4\omega_k^2}{(m^2 + q^2 + \omega_k^2)(m^2 + (p+q)^2 + \omega_k^2)} \,, \tag{B.8}$$

where we defined $\omega_k = 2\pi k/L$. Introducing again the Feynman parameter and making the same substitution one arrives at

$$\Pi_{00} = \sum_{k=-\infty}^{\infty} \frac{N\omega_k^2}{L} \int_0^1 \frac{dx}{(m^2 + \omega_k^2 + p^2 x(1-x))^{3/2}} \,. \tag{B.9}$$

We expand this expression and keep only the leading power in p. Then the expression for the charge becomes

$$\begin{aligned}\frac{1}{Ne^2} &= \frac{1}{4L}\left[\sum_{k=-\infty}^{\infty}(m^2+\omega_k^2)^{-3/2} - m^2\sum_{k=-\infty}^{\infty}(m^2+\omega_k^2)^{-5/2}\right] \\ &= \frac{L^2}{32\pi^3}\left[\sum_{k=-\infty}^{\infty}(k^2+\alpha^2)^{-3/2} - \alpha^2\sum_{k=-\infty}^{\infty}(k^2+\alpha^2)^{-5/2}\right], \qquad \text{(B.10)}\end{aligned}$$

where $\alpha = Lm/2\pi$. We deal with these sums as follows:

$$\begin{aligned}S_1(z,\alpha) &\equiv \sum_{k=-\infty}^{\infty}(k^2+\alpha^2)^{-z} \overset{(A.4)}{=} \frac{1}{\Gamma(z)}\int_0^\infty dt\, t^{z-1}e^{-t\alpha^2}\sum_{k=-\infty}^{\infty}e^{-k^2t} \\ &\overset{(A.7)}{=} \frac{1}{\Gamma(z)}\int_0^\infty dt\, t^{z-1}e^{-t\alpha^2}\Theta_3(0,it/\pi) \\ &\overset{(A.8)}{=} \frac{\sqrt{\pi}}{\Gamma(z)}\int_0^\infty dt\, t^{z-1}e^{-t\alpha^2}\Theta_3(0,-\pi/it) \\ &\overset{(A.6)}{=} \frac{\sqrt{\pi}}{\Gamma(z)}\left[\frac{\Gamma(z-\frac{1}{2})}{\alpha^{2z-1}} + 4\sum_{k=1}^{\infty}\left(\frac{k\pi}{\alpha}\right)^{z-\frac{1}{2}}K_{z-\frac{1}{2}}(2k\pi\alpha)\right]. \qquad \text{(B.11)}\end{aligned}$$

Thus the expression for the charge can be written as

$$\begin{aligned}\frac{1}{Ne^2} &= \frac{1}{4L}\left(\frac{L}{2\pi}\right)^3\left[S_1(3/2,\alpha) - \alpha^2 S_1(5/2,\alpha)\right] \\ &= \frac{1}{12\pi m^2} + \frac{L}{2\pi m}\sum_{k=1}^{\infty}K_1(kLm)\,k - \frac{L^2}{6\pi}\sum_{k=1}^{\infty}K_2(kLm)\,k^2. \qquad \text{(B.12)}\end{aligned}$$

In the limit $Lm \gg 1$ the contributions from the modified Bessel functions are exponentially small and thus the expression for the charge reduces to that for the infinitely long string.

Appendix C

Kinetic term in the supersymmetric case

In Appendix B we calculated the first diagram (the boson part) in Fig. 3.6. Now we will calculate the second diagram (the fermion part). The relevant part of the fermion action in the Minkowski spacetime is

$$\begin{aligned} iS_F^M &= i\int d^2x\Bigg\{\bar{\xi}\, i\gamma^\mu\nabla_\mu\,\xi - i\sqrt{2}\sigma\bar{\xi}\left(\frac{1-\gamma^5}{2}\right)\xi \\ &+ i\sqrt{2}\sigma^*\bar{\xi}\left(\frac{1+\gamma^5}{2}\right)\xi\Bigg\}, \end{aligned} \tag{C.1}$$

where $\nabla_\mu = \partial_\mu - iA_\mu$ is the covariant derivative, and the γ matrices are defined as

$$\gamma^0 = \begin{pmatrix} 0 & -i \\ i & 0 \end{pmatrix}, \quad \gamma^1 = \begin{pmatrix} 0 & i \\ i & 0 \end{pmatrix}, \quad \gamma^5 = \begin{pmatrix} 1 & 0 \\ 0 & -1 \end{pmatrix}.$$

We pass to Euclidean space,

$$t = -i\tau\,, \quad A_0 = i\hat{A}_0\,, \quad A_i = \hat{A}_i\,, \quad \hat{\gamma}^0 = \gamma^0\,, \quad \hat{\gamma}^1 = -i\gamma^1\,, \quad \hat{\gamma}^5 = \gamma^5\,,$$

and, since in Euclidean formulation ξ and $\bar{\xi}$ are independent, we define

$$\hat{\xi} = \xi\,, \quad \hat{\bar{\xi}} = i\bar{\xi}\,.$$

Thus, the action in Euclidean space can be presented as follows:

$$\begin{aligned} S_F^E &= -\int d^2\hat{x}\left[\hat{\bar{\xi}}\, i\hat{\gamma}^k\hat{\partial}_k\,\hat{\xi} + \hat{\bar{\xi}}\,\hat{\gamma}^k\hat{A}_k\,\hat{\xi}\right. \\ &- \left.\sqrt{2}\sigma\hat{\bar{\xi}}\left(\frac{1-\hat{\gamma}^5}{2}\right)\hat{\xi} + \sqrt{2}\sigma^*\hat{\bar{\xi}}\left(\frac{1+\hat{\gamma}^5}{2}\right)\hat{\xi}\right]. \end{aligned} \tag{C.2}$$

Examining this expression in components one can find that it matches that of (3.5.2). Since from now on all calculations will be carried out in Euclidean space we will drop the caret notation. Using (C.2) we find the Feynman rules that are shown in Fig. (C.1), where we introduced a notation $\sigma = a + ib$ and the mass is $m^2 = 2a^2 + 2b^2$.

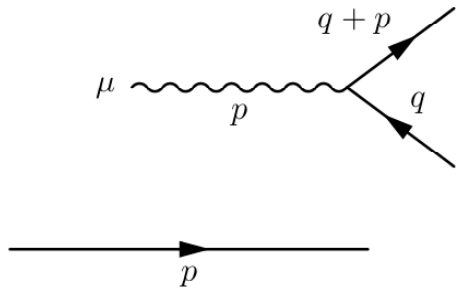

$$= \gamma^\mu$$

$$= \frac{\not{p} + ib\sqrt{2} + a\sqrt{2}\gamma^5}{p^2+m^2}$$

Figure C.1: Feynman rules: vertex and the propagator of ξ^l field.

We begin from the case of the infinitely long string. The fermion contribution to the kinetic term is

$$\begin{aligned} \Pi^{ij} &= -\int \frac{d^2q}{(2\pi)^2}\frac{1}{(q^2+m^2)[(p+q)^2+m^2]} \\ &\times \mathrm{Tr}\left[\gamma^i(\not{q} + i\sqrt{2}b + \sqrt{2}a\gamma^5)\gamma^j(\not{p}+\not{q} + i\sqrt{2}b + \sqrt{2}a\gamma^5)\right]. \end{aligned} \tag{C.3}$$

The Clifford algebra is, as usual,

$$\{\gamma^i\gamma^j\} = 2\delta^{ij}\,. \tag{C.4}$$

As a result, the trace identities for the γ matrices become

$$\begin{aligned} \mathrm{Tr}(\gamma^i\gamma^j) &= 2\delta^{ij}\,, \\ \mathrm{Tr}(\gamma^i\gamma^j\gamma^k\gamma^l) &= 2\delta^{ij}\delta^{kl} - 2\delta^{ik}\delta^{jl} + 2\delta^{il}\delta^{jk}\,, \\ \mathrm{Tr}(\text{odd number of }\gamma\text{'s}) &= 0\,. \end{aligned} \tag{C.5}$$

Thus, the expression for the kinetic term takes the form

$$\begin{aligned} \Pi^{ij} &= -\int \frac{d^2q}{(2\pi)^2} \frac{\mathrm{Tr}[\gamma^i \not{q} \gamma^j (\not{p}+\not{q}) - m^2\gamma^i\gamma^j]}{(q^2+m^2)[(p+q)^2+m^2]} \\ &= -\int \frac{d^2q}{(2\pi)^2} \frac{1}{(q^2+m^2)[(p+q)^2+m^2]} \\ &\times \quad [2q^i(p+q)^j + 2q^j(p+q)^i - 2q\dot{(}p+q)\delta^{ij} - 2m^2\delta^{ij}]\,. \end{aligned} \tag{C.6}$$

Notice, that generally speaking $\mathrm{Tr}(\gamma^i\gamma^j\gamma^5) \neq 0$ in two dimensions. However, we find that both such contributions cancel each other.

We proceed as in the bosonic theory, introducing the Feynman parameter and making the same substitution. Linear terms drop out, as usual. Furthermore, considering only p^ip^j structure we obtain

$$\begin{aligned} \Pi_F^{ij} &= p^ip^j \int \frac{d^2l dx}{(2\pi)^2} \frac{1-(1-2x)^2}{(l^2+m^2+p^2x(1-x))^2} \\ &= p^ip^j \int_0^1 \frac{dx}{4\pi} \frac{1-(1-2x)^2}{m^2+p^2x(1-x)}\,. \end{aligned} \tag{C.7}$$

Expanding to zeroth order in p we find fermion contribution to e^2 ,

$$\frac{1}{Ne_F^2} = \frac{1}{6\pi m^2}\,. \tag{C.8}$$

Combining this with the result we obtained in the boson theory, we finally arrive at

$$\frac{1}{Ne^2} = \frac{1}{4\pi m^2}\,. \tag{C.9}$$

In the case of the finite length string the starting expression (C.6) is modified

$$\begin{aligned} \Pi^{ij} &= -\frac{1}{L}\sum_{k=-\infty}^{\infty} \int \frac{dq}{2\pi} \frac{1}{(q^2+m^2)[(p+q)^2+m^2]} \\ &\times \quad [2q^i(p+q)^j + 2q^j(p+q)^i - 2q\dot{(}p+q)\delta^{ij} - 2m^2\delta^{ij}]\,. \end{aligned} \tag{C.10}$$

Again, just as in the boson theory we consider Π_{00}. After we make the same substitution and introduce the Feynman parameter we obtain

$$\Pi_{00} = \frac{m^2}{L} \sum_{k=-\infty}^{\infty} \int_0^1 \frac{dx}{(p^2 x(1-x) + m^2 + \omega_k^2)^{3/2}} \,. \tag{C.11}$$

Then we expand this expression and keep only the first nonvanishing power in p. Thus, fermionic contribution to the charge is

$$\frac{1}{Ne_F^2} = \frac{m^2}{4L} \sum_{k=-\infty}^{\infty} (m^2 + \omega_k^2)^{-5/2} \tag{C.12}$$

Summarizing, we obtained a sum identical to that in (B.10). Therefore, their evaluation is identical too. Combining the result found in this Appendix with that of the boson theory, we obtain for the charge

$$\frac{1}{Ne^2} = \frac{1}{4\pi m^2} + \frac{L}{2\pi m} \sum_{k=1}^{\infty} K_1(Lmk)k \,. \tag{C.13}$$

Appendix D

Relations for modified Bessel functions

In this Appendix we derive all the relations for the sums of modified Bessel functions of the second kind used in the text. We will use the following asymptotic behavior

$$K_1(z) \to \frac{1}{z} \quad \text{as} \quad z \to 0\,, \tag{D.1}$$

as well as the properties of derivatives

$$K_0(z)' = -K_1(z) \quad \text{and} \quad K_1'(z) = -K_0(z) - \frac{K_1(z)}{z}\,, \tag{D.2}$$

and the following approximations, valid to order $O(y^2, z^2)$ (see formula 8.526 in [42])

$$\begin{aligned} \sum_{k=1}^{\infty} K_0(zk)\cos(yk) &= \frac{\gamma}{2} + \frac{1}{2}\ln\frac{z}{4\pi} + \frac{\pi}{2\sqrt{z^2+y^2}} + S_0(2y^2 - z^2) + \delta_0\,, \\ \sum_{k=1}^{\infty} K_0(zk)(-1)^k\cos(yk) &= \frac{\gamma}{2} + \frac{1}{2}\ln\frac{z}{4\pi} + \frac{S_1}{2} + \frac{S_2}{2}(2y^2 - z^2) + \delta_1\,, \end{aligned} \tag{D.3}$$

where $\delta_{0,1} \sim y^2 z^2$ and we defined the sums

$$\begin{aligned} S_0 &= \sum_{l=1}^{\infty} \frac{\pi}{(2\pi l)^3} \approx 0.015\,, \quad S_1 = \sum_{l=1}^{\infty} \frac{1}{l(2l-1)} \approx 1.386\,, \\ S_2 &= \sum_{l=1}^{\infty} \frac{1}{\pi^2(2l-1)^3} \approx 0.107\,. \end{aligned} \tag{D.4}$$

To find the sum involving cosine we notice that on one hand

$$\frac{d}{dz}\left(z\sum_{k=1}^{\infty}\frac{K_1(zk)}{k}\cos(yk)\right)=-z\sum_{k=1}^{\infty}K_0(zk)\cos(yk)\,, \tag{D.5}$$

and on the other hand

$$\frac{d}{dy}\left(\sum_{k=1}^{\infty}\frac{K_1(zk)}{k}\cos(yk)\right)=-\sum_{k=1}^{\infty}K_1(zk)\sin(yk)\,, \tag{D.6}$$

moreover the following relation also holds

$$\frac{d}{dz}\left(\sum_{k=1}^{\infty}K_0(zk)\cos(yk)\right)=-\frac{d}{dy}\left(\sum_{k=1}^{\infty}K_1(zk)\sin(yk)\right)\,, \tag{D.7}$$

where we used (D.2) several times.

First using (D.5) and the expansion from (D.3) we find to order $O(y^2,z^2)$

$$\begin{aligned}\sum_{k=1}^{\infty}\frac{K_1(zk)}{k}\cos(yk) &\approx -\frac{\pi\sqrt{z^2+y^2}}{2z}-\frac{z(2\gamma-1)}{8}-\frac{z}{4}\ln\frac{z}{4\pi}\\ &- S_0zy^2+\frac{f_1(y)}{z}\end{aligned} \tag{D.8}$$

where $f_1(y)$ depends on y.

Now using (D.7) and approximation (D.3) we find that

$$\sum_{k=1}^{\infty}K_1(zk)\sin(yk)\approx\frac{\pi y}{2z\sqrt{z^2+y^2}}-\frac{y}{2z}+2S_0zy+f_2(z)\,, \tag{D.9}$$

where $f_2(z)$ is a function which depends on z. Since LHS vanishes when $y=0$ and $z\neq 0$ we conclude that $f_2(z)=0$. Now from (D.6) we find that

$$\sum_{k=1}^{\infty}\frac{K_1(zk)}{k}\cos(yk)\approx-\frac{\pi\sqrt{z^2+y^2}}{2z}+\frac{y^2}{4z}-S_0zy^2+f_3(z)\,, \tag{D.10}$$

where $f_3(z)$ depends on z.

To fix $f_1(y)$ and $f_3(z)$ we use the property (D.1) and find that

$$\sum_{k=1}^{\infty}\frac{K_1(zk)}{k}\cos(yk)\to\sum_{k=1}^{\infty}\frac{\cos(yk)}{zk^2}=\frac{1}{z}\left(\frac{y^2}{4}-\frac{\pi y}{2}+\frac{\pi^2}{6}\right)\,. \tag{D.11}$$

Thus we conclude that

$$\begin{aligned}\sum_{k=1}^{\infty}\frac{K_1(zk)}{k}\cos(yk) &\approx -\frac{\pi\sqrt{z^2+y^2}}{2z}+\frac{y^2}{4z}+\frac{\pi^2}{6z}-S_0zy^2\\ &- \frac{z(2\gamma-1)}{8}-\frac{z}{4}\ln\frac{z}{4\pi}\,.\end{aligned}\tag{D.12}$$

In a similar way we find that

$$\begin{aligned}\sum_{k=1}^{\infty}\frac{K_1(zk)}{k}(-1)^k\cos(yk) &\approx -\frac{z(2S_1+2\gamma-1)}{8}-\frac{z}{4}\ln\frac{z}{4\pi}\\ &- \frac{\pi^2}{12z}+\frac{y^2}{4z}-\frac{S_2}{2}zy^2\,.\end{aligned}\tag{D.13}$$

Appendix E

Photon mass

In this Appendix we derive an expression for the photon mass. Due to gauge invariance both the diagrams in Fig. (4.7) have to be of the form

$$\Pi_{ij} = \Pi(p^2)\left(p^2\delta_{ij} - p_i p_j\right) . \tag{E.1}$$

Below we show that for the second diagram $\Pi(p^2)$ has a pole which means that photons acquire mass. We put $p_1 = 0$ and evaluate Π_{11}:

$$\begin{aligned}\Pi_{11} &= -\frac{1}{L}\Big[\sum_{k=-\infty}^{\infty}\int_{-\infty}^{\infty}\frac{dq_0}{2\pi}\frac{2q_1^2 - 2q_0(p_0+q_0) - 2m_1^2}{(q_0^2+q_1^2+m_1^2)(p_0^2+2p_0q_0+q_0^2+q_1^2+m_1^2)} \\ &- [m_1 \leftrightarrow m_2]\Big] ,\end{aligned} \tag{E.2}$$

where m_1 is the fermion mass, which we put to zero at the end, m_2 is the mass of Pauli-Villars regulator, and q_1 is a discrete momentum

$$q_1 = \frac{2\pi k}{L} + A_1 = \frac{\pi}{L}\left(2k+1\right) . \tag{E.3}$$

We introduce Feynman parameter x and substitute integration variable $q_0 = l - p_0 x$

$$\Pi_{11} = -\frac{1}{L}\Big[\sum_{k=-\infty}^{\infty}\int_{-\infty}^{\infty}\int_0^1\frac{dldx}{2\pi}\frac{2q_1^2 - 2m_1^2 + 2p_0^2x(1-x) - 2l^2}{[l^2+m_1^2+q_1^2+xp_0^2-x^2p_0^2]^2} - [m_1 \leftrightarrow m_2]\Big] , \tag{E.4}$$

where terms linear in l drop out. Integrating over l one finds

$$\Pi_{11} = \frac{1}{L}\Big[\sum_{k=-\infty}^{\infty}\int_0^1 dx\frac{m_1^2}{[m_1^2+q_1^2+xp_0^2-x^2p_0^2]^{3/2}} - [m_1 \leftrightarrow m_2]\Big] , \tag{E.5}$$

and since $m_1 = 0$ the first term vanishes and only the contribution from the regulator remains. To integrate over x we use third Euler's substitution

$$\sqrt{-p_0^2 x^2 + p_0^2 x + m^2 + q_1^2} = \sqrt{-p_0^2 (x - x_1)(x - x_2)} = t(x - x_1)\,. \tag{E.6}$$

One can easily check that neither of the roots belong to the interval $x \in [0, 1]$ and thus this substitution is justified. After integration we obtain the following sum

$$\Pi_{11} = -\frac{1}{L} \sum_{k=-\infty}^{\infty} \frac{m_2^2}{(q_1^2 + m_2^2 + \frac{p_0^2}{4})\sqrt{q_1^2 + m_2^2}} \approx -\frac{1}{L} \sum_{k=-\infty}^{\infty} \frac{m_2^2}{(q_1^2 + m_2^2)^{3/2}}\,, \tag{E.7}$$

where we ignore p_0 compared to m_2. Evaluating this sum (see Appendix B) we finally obtain (setting $m_2 \to \infty$)

$$\Pi_{11} = -\frac{1}{\pi}\,, \tag{E.8}$$

which tells us that $\Pi(p^2)$ indeed contains a pole

$$\Pi(p^2) = -\frac{1}{\pi p^2} \tag{E.9}$$

and the photon becomes massive.